Experimental Constraints on Fe Concentrations in Biomass Burning Aerosols

by

Alyssa M Sherry

A Thesis Presented in Partial Fulfillment
of the Requirements for the Degree
Master of Science

Approved April 2019 by the
Graduate Supervisory Committee:

Ariel Anbar, Co-Chair
Pierre Herckes, Co-Chair
Hilairy Hartnett
Matthew Fraser

ARIZONA STATE UNIVERSITY

May 2019

ABSTRACT

Atmospheric deposition of iron (Fe) can limit primary productivity and carbon dioxide uptake in some marine ecosystems. Recent modeling studies suggest that biomass burning aerosols may contribute a significant amount of soluble Fe to the surface ocean. Existing studies of burn-induced trace element mobilization have often collected both entrained soil particles along with material from biomass burning, making it difficult to determine the actual source of aerosolized trace metals.

In order to better constrain the importance of biomass versus entrained soil as a source of trace metals in burn aerosols, small-scale burn experiments were conducted using soil-free foliage representative of a variety of fire-impacted ecosystems. The resulting burn aerosols were collected in two stages (PM > 2.5 μm and PM < 2.5 μm) on cellulose filters using a high-volume air sampler equipped with an all-Teflon impactor. Unburned foliage and burn aerosols were analyzed for Fe and other trace metals using inductively coupled plasma mass spectrometry (ICP-MS).

Results of this analysis show that less than 2% of Fe in plant biomass is likely mobilized as atmospheric aerosols during biomass burning events. The results of this study and estimates of annual global wildfire area were used to estimate the impact of biomass burning aerosols on total atmospheric Fe flux to the ocean. I estimate that foliage-derived Fe contributes 114 ± 57 Gg annually. Prior studies, which implicitly include both biomass and soil-derived Fe, concluded that biomass burning contributes approximately 690 Gg of Fe. Together, these studies suggest that fire-entrained soil particles contribute 83% (576 Gg) of Fe in biomass burning emissions, while plant derived iron only accounts for at most 17%.

DEDICATION

This work is dedicated to my unwavering support system. Mom and Dad, thank you for always believing in me even when I don't believe in myself. Ariel Sherry, you always manage to keep me grounded and entertained, even when I don't want to be. My youngest siblings Anthony and Ashley, thank you for keeping my old soul young at heart. Grandma Donna and Grandma Pat, I'm sorry my trips home have been (too) short. I promise it's worth it. Grandpa John, I wish you could be here with me. I hope I made you proud. Your love means more to me than words can express.

The amazing women I call friends: you prop me up, push me further, and encourage me to be the best version of myself. I love you all, and I couldn't have done any of this without you. Aleisha Johnson, I couldn't have asked for a better lab sister and confidante. Genevieve Studer-Ellis, thank you for caring so much for my mental and emotional well-being (late-night taco runs included). Zee Wilson, I look forward to laughing with you until we're out of air. Sravani Vadlamani, thank you for teaching me how to say "no" without apology. Samantha Hernandez, you are a complete inspiration every day. My treasured adventure buddy, coffee compatriot, and shopping partner, Claire Crowther: what would I have done without you? Last, but certainly not least, Sierra Ferguson, my sister from another mister, kitchen tornado, and all-around nerd. You have truly made these the best five years of my life so far.

To the many people of GPSA and graduate students in chemistry and geology who have become my friends throughout this journey: thank you for lending a sympathetic ear over coffee and helping me decompress at happy hour. You are wonderful people and I am truly grateful for each and every one of you.

ACKNOWLEDGMENTS

This research would not be possible without the support of many incredible people. First and foremost, I would like to thank the staff of the Keck Environmental Lab at ASU. The tireless work of Gwyneth Gordon, Trevor Martin, and several student assistants in maintaining a safe, clean, functioning trace metal clean lab was absolutely critical for the success of my sample preparation and analysis, as well as the safety of my eyes and fingers. Their hard work and devotion do not go unnoticed or unappreciated.

Thank you so much Dr. Chad Geelhood for allowing me to use the Field Lab on Polytechnic Campus for my experiments. Thank you as well Dr. Joost van Haren at Biosphere 2 and Raul Puente Martinez at the Desert Botanical Garden for facilitating my sample collection and sweating through the Arizona heat with me. Further thanks to Logan Tegler and Sierra Ferguson for their assistance in sample collection.

I would also like to thank Stephen Romaniello for being a wicked mentor. His knowledge and patience were critical to all aspects of my work, including designing, setting up, collecting and transporting equipment and samples. He was always ready and willing to help analyze data or fix instruments. There are no words to describe how thankful I am for him.

Many thanks to my committee Dr. Pierre Herckes, Dr. Ariel Anbar, Dr. Hilairy Hartnett, and Dr. Matthew Fraser for their feedback, support, and thought-provoking questions throughout my time as a graduate student. Thank you for pushing me to become a better researcher.

TABLE OF CONTENTS

APPENDIX Page

LIST OF TABLES

Table Page

LIST OF FIGURES

CHAPTER 1

INTRODUCTION

The global carbon cycle depends upon the productivity of photosynthetic organisms. Marine primary producers called phytoplankton convert atmospheric carbon dioxide into 45 gigatons (Gt) of organic carbon annually.[1] Phytoplankton depend upon macronutrients such as nitrate, phosphate, and silicate. However, even when there is a sufficient supply of these macronutrients, phytoplankton productivity may be limited in areas termed "high nutrient, low chlorophyll (HNLC)," which constitute approximately 25% of the surface ocean.[2] It is believed that HNLC areas lack sufficient concentrations of micronutrients, such as Fe. Iron facilitates electron transport in the mitochondria and chloroplasts of phytoplankton cells.[3] Therefore, without a sufficient supply of Fe, phytoplankton cannot perform photosynthesis. Therefore, biogeochemical models of marine productivity and atmospheric carbon dioxide must account for all sources of Fe to the surface ocean.

There are several known sources of Fe to the surface ocean.[4] Upwelling in Equatorial regions and the Southern ocean supplies Fe-rich deep water to the surface.[5] Water along continental margins may also experience upwelling and/or sediment dissolution, which releases Fe into the surrounding waters.[6–8] However, these processes do not impact the surface waters of much of the open ocean. In these areas, atmospheric deposition of particles is considered to be the most important source of Fe.[7,9,10]

Atmospheric particles, in turn, may be derived from mineral dust or combustion, like anthropogenic activity or biomass burning events. Mineral dust contributes approximately 12 Tg of Fe annually to the ocean – significantly more Fe than combustion

processes.[11] However, Fe in these particles is highly insoluble in ocean water, with some studies reporting Fe solubility of less than 1%.[12] Because of this insolubility, most of the Fe in mineral dust may not be readily available to phytoplankton (i.e., bioavailable).

Conversely, combustion aerosols only contribute 660-690 Gg of Fe to surface waters.[11,13] While this represents less total Fe than mineral dust, combustion aerosols are far more soluble, with measured Fe solubilities between 0.7-13%.[11,14] This may be due to the size and residence time of these particles. Combustion aerosols, on average, are typically < 1 μm in diameter, and thus are much smaller than dust aerosols, which may have diameters > 10 μm.[2] Therefore, combustion aerosols have higher surface-area-to-volume ratios and longer atmospheric residence times. Both of these factors allow more atmospheric processing of aerosols by acidic gases, which increases particle solubility.[15] According to recent modeling studies, up to 60% of the soluble Fe in the eastern Pacific and Southern Oceans, two HNLC areas is derived from combustion processes.[16,17]

Because of these differences in solubility, it is important to determine the relative importance of the sources of marine aerosols. Several methods currently exist to differentiate mineral dust and combustion aerosols from each other. Anthropogenic aerosols are differentiated based on the presence of elements such as vanadium and lead. The most prevalent tracers for biomass burning include levoglucosan and soluble potassium (K^+) because both are released in abundance during biomass burning events.[18,19] However, significant issues exist with these methods. Levoglucosan has been shown to degrade on the timescale of hours under typical atmospheric conditions.[20] For example, K^+ is also found in sea spray aerosol and therefore requires a correction factor.[18] Therefore, a new tracer is needed that more accurately source apportions Fe in aerosols.

One potential aerosol tracer is Fe isotopes, as various chemical reactions may fractionate isotopes of Fe uniquely. Isotopic fractionation has been studied for over 70 years and is the foundation of the field of stable isotope geochemistry.[21] Until the development of the multiple collector inductively-coupled plasma mass spectrometer (MC-ICP-MS), isotope fractionation measurements were only practical for light elements such as carbon and oxygen. The development of MC-ICP-MS has facilitated the measurement of isotopes of heavier elements, such as Fe.

Researchers recently began using variations in Fe isotope values to apportion sources of marine aerosols. Mead and others[22] collected aerosols in Bermuda and analyzed their Fe concentration and Fe isotopes. They determined that aerosols primarily originating in the Sahara had Fe isotope compositions resembling mineral dust. In months outside of this "Saharan season," the aerosols had distinctly lighter Fe isotope values, indicating a non-mineral dust source. They concluded that this isotopically light source could be biomass burning, as studies by Guelke and von Blanckenburg indicated that Fe taken up by some plants was isotopically lighter than the soil in which the plant was grown.[23–26] Recent studies by Kurisu and others[14,27–29] indicate that combustion aerosols may also contain light Fe. These studies measured Fe isotopes in combustion aerosols from anthropogenic activity and discovered Fe isotope compositions much lighter than those observed by Majestic and others.[30]

Further studies by Kurisu and Takahashi[14] found that Fe in biomass burning aerosols is isotopically indistinguishable from mineral dust. This aligns with other studies that posit most of the Fe in biomass burn aerosols is derived from lofted soil particles from uplifting air currents and burning duff during floor fires.[11,31] Thus, these aerosols

may have Fe isotope compositions similar to mineral dust. If lofted soil particles are the primary source of Fe in biomass burning aerosols, then aerosols from natural sources (mineral dust and biomass burning) would have similar isotope values. If, on the other hand, a substantial amount of Fe comes from burning foliage (crown fires), then these aerosols may show light isotope ratios. However, no studies have directly measured the isotopic composition of burning foliage in biomass burning aerosols. In addition, the contribution of Fe from burning foliage vs lofted soil has not yet been quantified.

Measurements of Fe in biomass burning aerosols are hindered by low Fe concentrations (as low as 0.0045 ± 0.026% of collected aerosol mass).[32] The most obvious solution to this challenge is to increase the amount of material burned. However, doing so raises some significant issues. First, burning more material would increase the total number of particles, most of which are organic or black carbon. Because many studies of trace metals in aerosols use cellulose filters which may clog when too much material is collected, there is a limit to how many aerosol particles may be collected. Second, burning more material also increases the temperature dramatically. The intake air frequently reached above 175 ˚C, and cellulose filters ignite at 233˚C. Even keeping the temperature below 175 ˚C, cellulose filters become very brittle. Therefore, there is a risk of damaging the cellulose filters if more material is burned in experiments.

Additionally, measurements of trace metals in biomass burning aerosols are limited by available facilities. Current fire lab facilities are designed to capture and study organic materials, not trace metals. These facilities use metal ductwork, stages, and other Fe-containing components.[33,34] Thus, the background contribution of Fe may exceed the concentration in collected aerosols. For example, Brian Majestic at the University of

Denver received samples from the U. S. Forest Service Fire Science Laboratory (FSL) in Missoula, Montana. However, these samples were only one half of a 1" diameter Teflon filter, and did not contain more Fe than the background [personal communication].

To overcome these challenges and collect a substantial amount of Fe, I developed rigorous experimental methods. I determined the maximum amount of material that could be burned without overloading the filters, and added this material to the fuel bed in small increments to keep the temperature under 175 ˚C. In addition, I used aluminum ductwork and a Teflon stage to minimize aerosol contact with Fe-containing materials. I also developed rigorous filter cleaning protocols (detailed in Appendix A) and foliage sample cleaning methods to reduce the amount of Fe-rich soil adhered to the foliage. Additionally, I minimized the impact of anthropogenic and mineral dust aerosols by conducting all burn experiments in an isolated location on a tarp.

These procedures enabled me to conduct biomass burning experiments and quantify the amount of Fe released from burning foliage during these events. I use these analyses to estimate the annual flux of Fe that comes from burning foliage versus entrained soil. This, in turn, could help us to determine if Fe isotopes are appropriate to use to distinguish sources of Fe in atmospheric particles.

CHAPTER 2

EXPERIMENTS

1. INTRODUCTION

Iron (Fe) is important to the carbon cycle and global ocean productivity, as it is a critical micronutrient for phytoplankton in the surface ocean. Constraints on marine primary productivity in high-nutrient, low-chlorophyll (HNLC) regions, which constitute as much as 25% of the open ocean, are attributed to limited bioavailability of Fe.[35–37] In HNLC areas, Fe concentrations fall below 0.2 nM.[38] An influx of Fe to HNLC areas of the Southern Ocean and equatorial Pacific has been shown to induce phytoplankton blooms.[39–41] Due to phytoplankton's impact on the global carbon cycle, it is necessary to identify and quantify all sources of Fe to the marine environment.

While Fe is supplied to the ocean from several sources, few may increase open ocean phytoplankton productivity. While Fe may be supplied to some marine areas by hydrothermal vents and sediment dissolution,[6,8,42–47] atmospheric particle deposition contributes the greatest flux of Fe to the surface waters of the open ocean.[9,10,48] Mineral dust aerosols make up approximately 98% of these particles.[11] However, the Fe in mineral dust may have solubilities as low as 1%,[49] thus most of Fe in mineral dust is not readily available to phytoplankton, or "bioavailable".

In contrast, Fe in combustion aerosols from anthropogenic emissions and biomass burning events are more soluble,[17,49,50] and thus provide a substantial amount of bioavailable Fe to the open ocean.[51] Combustion aerosols have large surface-area-to-volume ratios and long atmospheric residence times, which promotes breakdown by acidic atmospheric gases.[15,18,52–54] A recent modeling study estimated that combustion

aerosols supply up to 50 Gg/yr of soluble Fe to the ocean, representing 15% of the total global soluble Fe flux from atmospheric particles.[17] This study suggests that biomass burning aerosols, in particular, contribute up to 60% of the soluble Fe in certain HNLC regions, such as the Southern Ocean.

Recent studies have suggested that the Fe in biomass burning aerosols is primarily derived from soil suspension due to uplifting air currents in the smoke plume[14,55] and burning duff, which consists of leaf litter, decomposing plant matter, and plant roots.[31,56] Studies of Fe in aerosols produced during biomass burning may help quantify the amount of Fe from burning foliage in biomass burning aerosols. However, no studies have directly measured the amount of Fe derived from burning foliage.

In this study, small-scale burn experiments were conducted to determine the amount of Fe released from burning foliage. The results of these experiments were used to estimate the contribution of burning foliage to the global flux of aerosol Fe released from biomass burning events annually.

2. MATERIALS AND METHODS

Clean foliage was burned, and the resulting aerosols were collected on cellulose filters via a modified high-volume sampler (Figures 4-6). These filters were digested and analyzed for their Fe content. Details provided in the following subsections include (1) reagent and material preparation, (2) sample collection, (3) burn experiment procedures, (4) sample processing, (5) sample analysis, and (6) blanks.

2.1 Reagent and material preparation

In anticipation of low Fe concentrations, reagents and materials were chosen and/or cleaned to avoid possible contamination. Laboratory procedures were conducted

in a Class 10 laminar flow hood. Unless otherwise specified, acids used in this study were purified via sub-boiling in-house distillation, and concentrated acids were diluted using 18 MΩ-cm DI water. Plastics in contact with samples and reagents were first degreased in Micro90 trace metal cleaning solution (1%), rinsed with DI water, and sequentially soaked in reagent-grade HNO_3 (7.8 M), HCl (6.1 M), and DI water, using standard trace-metal clean lab protocols.[57] Polytetrafluoroethylene (PTFE, Teflon) containers were further cleaned by refluxing with concentrated HCl on a hotplate for 2-3 hours.

Full and slotted cellulose filters (203 x 254 mm (TE-241), 152 x 152 mm (TE-230-WH), Whatman 41, Tisch Env.) soaked overnight in reagent-grade HCl (0.24 M) and were rinsed with DI water three times. This process was repeated for a total of three wash cycles. Filters dried and were stored in plastic zipper bags. Filter handling was minimal, but during handling, gloves were worn and acid-washed PTFE tweezers were used.

2.2 Sample collection

Foliage samples were selected to represent plants in areas subject to frequent or intense biomass burning events. Pine needles sampled from the Coconino National Forest were selected as analogues for boreal biomes. Tropical foliage from Biosphere 2 was selected to represent various plants from humid, tropical biomes. Eucalyptus foliage from the Desert Botanical Garden was selected to typify arid tropical biomes. Grassland and croplands were represented by grass samples from Buffalo Park in Flagstaff, AZ.

One sample of each tree species outlined in Table 1 was collected from 1-2 m above ground and each grass sample was cut approximately two inches above the roots to minimize soil contact. These samples were rinsed three times in DI water and dried at 50 ºC in a standard laboratory oven. Pine needles, eucalyptus foliage, and grass herbage

were also rinsed with a methanol-water solution (50%) to remove particulates adhered to the outer waxy coating.[58] A small portion (1-2 g) of each foliage sample was analyzed for trace metal concentrations.

2.3 Burn experiment procedures

Clean foliage samples were burned outdoors on a secluded gravel lot located in Gilbert, AZ during three separate sessions (January 13, July 19, and September 1, 2017). Schematics and pictures of the experimental setup can be found in Appendix I. The setup was assembled on a tarp to prevent contamination by soil particles in the vicinity of the experiment. Aerosol samples were collected using a high-volume sampler, drawing air at approximately 1.13 m^3/min. Aluminum ductwork (4" diameter) was connected to the sampling stage (Figure A). The sampling stage was constructed out of a PTFE frame and mesh to reduce Fe transfer from the sampler to filters. This stage was soaked in reagent-grade HCl (2.4 M) overnight, rinsed, and dried prior to use. The stage was equipped with an aluminum cascade impactor to separate aerosols into fine (PM<2.5 μm) and coarse (PM>2.5 μm) modes. This study focuses on fine particles, as they have long atmospheric residence times and are more likely to deliver soluble Fe to the ocean.[27,28,49,59]

The fire bed was constructed using cinder blocks and a ceramic floor tile, which were covered in aluminum foil (Figure 5, Appendix I). Two cinder blocks were placed on the tarp to prevent melting. Aluminum sheeting and the ceramic floor tile were placed on top of the tarp for further insulation. This arrangement was surrounded by cinder blocks to prevent the fire from spreading to surrounding vegetation and structures. A new piece of aluminum foil was placed on top of the ceramic floor tile before each burn to prevent cross-contamination and to enable collection of post-burn ash.

Table 1: Sample details including species, total dry weight, and sampling location. Dry weights represent the weight of clean, dry foliage samples. A small portion (1-2 g) was set aside for elemental analysis. The remaining material was ignited in burn experiments.

Biome	Classification	Dry sample wt. (g)	Location collected
Temperate/Boreal	*Pinus ponderosa*	123.90	Coconino National Forest Sedona, AZ
	Pinus ponderosa	156.96	
	Pinus ponderosa	135.52	
	Pinus ponderosa	156.71	
Humid tropical	*Arenga pinnata*	82.67	Biosphere 2 Oracle, AZ
	Bambusa spp.	39.72	
	Cissus sicyoides	17.00	
	Costas spp.	23.33	
	Elaeis guianensis	102.06	
	Inga spp.	29.42	
	Melia azedarach	70.11	
	Musa spp.	41.31	
	Pachira aquatica	30.68	
	Spathodea campanulata	23.59	
Arid tropical	*Eucalyptus camaldulensis*	97.12	Desert Botanical Garden Phoenix, AZ
	Eucalyptus erythrocorys	165.57	
	Eucalyptus microtheca	108.14	
	Eucalyptus papuana	61.60	
	Eucalyptus woodwardii	101.53	
Grassland	*Pascopyrum smithii*	53.48	Buffalo Park Flagstaff, AZ
	Elymus elymoides	56.62	
	Thinopyrum intermedium	32.77	
	Bouteloua gracilis	38.96	
	Sorghastrum nutans	65.79	

At the beginning of each burn, small amounts of foliage were placed on the aluminum foil, sprayed with 1 mL of acetone, and ignited using matches. All matches were discarded after ignition, and thus were not burned with foliage. The sampler was turned on before ignition and turned off post-smoldering. To prevent damage to the PTFE sampler, air temperature was kept below 300 ˚C by gradually adding small amounts of foliage to the fuel bed until all sample was consumed. Occasionally, re-ignition using a small amount of acetone (< 1 mL) and matches was required. Each burn lasted four to ten minutes. Cellulose filters were collected from the sampling stage using acid-washed tweezers and returned to their zipper bags. Ash from the fire was wrapped in aluminum foil and secured in zipper bags in the field.

2.4 Sample processing

Sample digestion was conducted according to modified methods described in Upadhyay and others.[60] One to two grams of unburned foliage was placed into PTFE-lined glass digester vessels (35 mL, Discover SP-D, CEM) with concentrated HNO_3 (10 mL) and DI water (5 mL). These vessels were microwaved at 240 ºC for 15 min **[**full ramp procedures in Appendix B]. The volume of the resulting digest was transferred to a PTFE vial, reduced to < 5 mL on a hot plate, transferred back to the digestion vessel using concentrated HNO_3 (10 mL), re-digested, and dried to residue. Residues were subjected to a secondary hot plate digestion procedure, as follows: concentrated HNO_3 and 30% trace metal grade H_2O_2 (750:250 µL) for two hours; concentrated HNO_3 and HCl overnight (3:1 mL); concentrated HNO_3 and HF (4:1 mL) overnight; and concentrated HCl (5 mL) overnight. Between each step, sample containers were opened, and their volume was reduced to near-dryness.

One quarter of each filter was digested via microwave (25 mL MARSXpress vessels, MARS 5, CEM). Filters were cut using zirconia ceramic blades (Specialty Blades, Inc.) on an acid-washed polypropylene cutting board and handled using acid-washed PTFE tweezers. Samples were placed into digestion vessels with concentrated HNO_3 (10 mL), concentrated trace metal grade HF (1 mL), and DI water (4 mL). Digestion vessels were heated over 30 min to 180 ºC. The volume of the resulting digest was reduced to < 5 mL, transferred back into the digestion vessel with 10 mL HNO_3, re-digested, and dried to residue. The residue was treated with concentrated HNO_3 and 30% trace metal grade H_2O_2 (500:250 µL) over a hot plate for two hours.

An ash sample from each burn was digested via microwave (25 mL MARSXpress vessels, MARS 5, CEM). Samples were placed into digestion vessels with concentrated HNO_3 (10 mL) and DI water (4 mL). The volume of the resulting digest was reduced to < 5 mL on a hotplate, transferred back to the digestion vessel with 10 mL concentrated nitric acid, re-digested, and dried to residue. These samples then underwent a hot plate digestion procedure, as follows: concentrated HNO_3 and H_2O_2 (750:250 µL) for two hours in a closed vessel; aqua regia overnight (3:1 mL); concentrated HNO_3 and HF (4:1 mL) overnight; and, concentrated HCl (5 mL) overnight. Between each step, sample containers were opened, and their volume was reduced to near-dryness.

2.5 Sample analysis

An aliquot of each digest was diluted to 5 mL using HNO_3 (0.32 M) and analyzed for 42 major and minor elements using a quadrupole inductively-coupled plasma mass spectrometer (ICP-MS, iCAP Q, Thermo Scientific) at the W.M. Keck Foundation Laboratory for Environmental Biogeochemistry. He was used as a collision gas to

remove polyatomic interferences such as $^{40}Ar^{16}O^{+}$. An internal standard containing Sc, Ge, Y, In, and Bi was used to correct for instrumental drift throughout each run. The limit of detection for Fe measurements was < 6 ng L^{-1}. The precision of Fe measurements was ± 2% based on repeated measurements of standard solutions interspersed within each run.

2.6 Blanks

Several types of blank were collected during sampling and sample processing to account for all sources of Fe in the experiment. Fe concentrations of in-house distilled HNO_3 and HCl were 1.3 and 8.9 parts per trillion, respectively. Clean acid processed as a sample with each set of digestions was called the "reagent blank." The digestion of unburned materials had a reagent blank containing 393 ng Fe. The reagent blanks that accompanied burn aerosol samples contained < 195 ng of Fe. For each burn session, one quarter of two clean filters were digested as samples to evaluate the Fe contribution from the cellulose filter substrate. This blank was termed the "filter blank." Each blank had 1.1 – 2.5 μg of Fe per filter. To determine the Fe contribution from the sampling stage, one clean filter was placed in the PTFE sampling stage for 10 min without the air pump turned on and removed with PTFE tweezers. One quarter of this filter, termed the "contact blank," was processed as a sample. The Fe concentration of the contact blanks did not exceed the filter blanks. Particulate matter from the ambient air was collected on clean filters before, during (every three samples), and after each session for five to ten minutes and processed as a sample to determine the Fe contribution from ambient particulate matter. This blank was termed the "field blank". Concentrations of the field blanks are shown in white in Figure 2.

3. RESULTS AND DISCUSSION

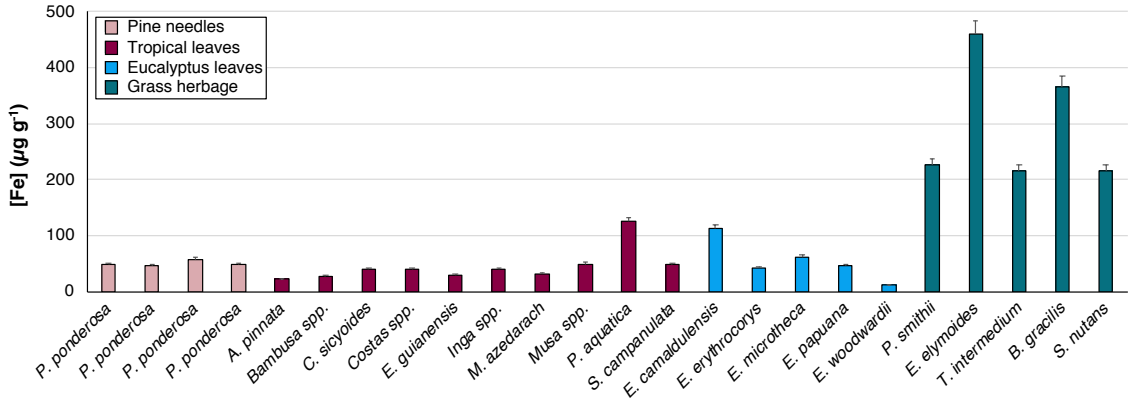

Figure 1: Amount of Fe concentrations in unburned foliage (μg_{Fe}) normalized to the dry weight (g_{DW}) of material analyzed. Error bars represent 5% of the measured value.

We conducted biomass burn experiments on 25 samples spanning four biomes. The Fe concentrations of unburned foliage samples are shown in Figure 1. In unburned pine, tropical, and eucalyptus foliage, 10-125 $\mu g_{Fe}/g_{DW}$ was measured, which is consistent with previous studies that measured 40-112 $\mu g_{Fe}/g_{DW}$.[61,62] Differences between the average Fe concentration in pine, tropical, and eucalyptus foliage were investigated using a one-factor analysis of variance (ANOVA). At the 95% confidence level, these three types of foliage are statistically indistinguishable ($p = 0.86$).

Grass samples have an average Fe concentration of 249.0 ± 35.2 $\mu g_{Fe}/g_{DW}$, which is significantly more Fe compared to the other types of plant material analyzed (ANOVA, $p < 0.05$). In addition, this is slightly higher than Fe concentrations measured by Schlegel and others[63] of 207.1 ± 208.1 $\mu g_{Fe}/g_{DW}$. The grass samples analyzed in this study were collected in Buffalo Park, Flagstaff, where soils are rich in basaltic material due to the proximity of several dormant volcanoes. Because basalts weather more easily, plants grown in basaltic soils tend to have higher concentrations of Fe and other trace metals.[64]

The concentration of Fe in the grass herbage agrees with studies of the Fe concentration in grass shoots grown in basaltic soils.[65]

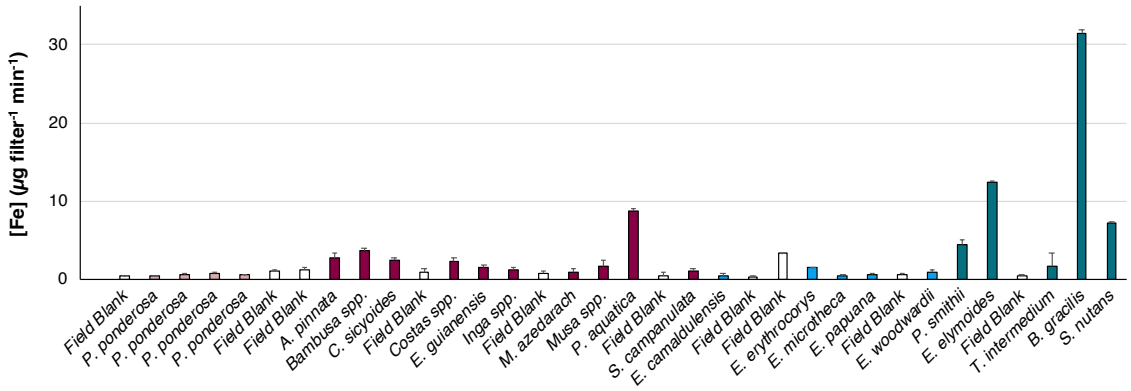

Figure 2: Concentrations of Fe in the filter blank corrected samples. The average measured concentration of Fe in unused, clean filters were subtracted from the measured amount of Fe in each filter. Error bars represent propagated error.

Figure 2 shows the amount of Fe in the fine particulate matter collected from each burn. Field blanks and burn aerosol samples were corrected for the contribution of Fe from the cellulose filter by subtracting the average amount of Fe in the filter blank (1.69 ± 1.45 μg filter^{-1}) from the amount of Fe in each field blank and burn aerosol sample. To compare field blanks and burn samples, each aerosol measurement was normalized for their respective particle collection times.

The concentrations in burned pine needle aerosol samples have an average and associated uncertainty of 0.56 ± 0.32 μg filter^{-1} min^{-1} (2σ). Because these samples were collected from the same tree at the same height, they may be considered replicates. Therefore, consistent amounts of Fe to be aerosolized between these samples are expected. When these samples are considered to be replicate measurements of the amount of Fe collected during the burning of replicate samples, the relative standard error of these measurements is approximately 29% (2σ). Replicate measurements of similar

biomass burning experiments conducted by the U. S. Forest Service's Fire Sciences Laboratory (FSL) at Missoula report a 16% (2σ) total error.[56] Unlike the FSL experiments, these experiments were conducted outside where air currents were less predictable. Therefore, a slightly larger relative standard error is expected.

The amount of Fe in the field blanks exceeds the amount of Fe in many burn aerosol samples. This could be a result of changing wind conditions bringing mineral dust aerosols into the setup. Because mineral dust aerosols have orders of magnitude more Fe than burn aerosols,[2,66] a small amount of mineral dust could have a significant effect on the amount of Fe collected on the filters. Despite this limitation, these measurements were utilized to determine the percentage of Fe aerosolized.

The percent of Fe that is aerosolized from unburned foliage during these burn experiments is estimated using the measured concentrations of Fe in the burn aerosols, field blanks, and unburned starting material, as shown in equation (1):

$$Fe_{aerosolized}(\%) = \left(\frac{Fe_{aerosol} - Fe_{field}}{Fe_{foliage}}\right) x\ 100 \qquad (1)$$

where $Fe_{aerosol}$ is the filter blank corrected amount of Fe in each sample in μg_{Fe} filter^{-1} min^{-1}, Fe_{fie} is the average field blank for each burn session in μg_{Fe} filter^{-1} min^{-1}, $Fe_{foliage}$ is the amount of Fe in the unburned foliage in μg_{Fe} per burn.

The results of this calculation are shown in Figure 3. No samples exceed 2% aerosolization of the Fe in the starting material. Several samples have slightly negative percentages of aerosolized Fe because these samples have Fe concentrations that are indistinguishable from their field blanks. Each value was weighted against its error, and a weighted average was calculated. The weighted average percent aerosolized, by sample

type, are -0.01 ± 0.01, 0.37 ± 0.09, -0.05 ± 0.04, and 0.06 ± 0.02 for pine, tropical, eucalyptus and grass samples, respectively. To take the weighted average, all of the samples within a given foliage type are assumed to be replicates and representative of the Fe content of that biome. These averages were used to estimate the impact of burning foliage on total biomass burning aerosols.

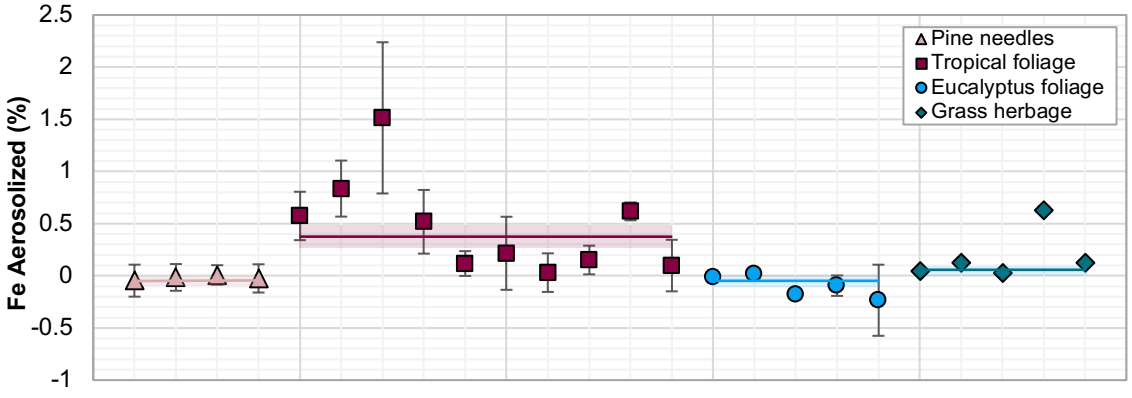

Figure 3: Percent of Fe aerosolized in PM<2.5 from the unburned foliage during biomass burning experiments. The average field blank has been subtracted from each sample. Error bars on the data points represent propagated error from the field blanks. Horizontal lines represent the weighted average, and shaded boxes represent the weighted error for each type of sample.

To assess the impact that burning foliage has on the global Fe flux from biomass burning aerosols, the percent of Fe aerosolized from burning foliage and the measured concentration of Fe in the unburned foliage were used, as shown in equation (2):

$$Fe\ flux = Fe_{aerosol}\ x\ Fe_{foliage}\ x\ density_{fuel}\ x\ area_{burned} \quad (2)$$

where $Fe_{aerosol}$ is the percent of Fe aerosolized during foliage burning, $Fe_{foliage}$ is the Fe concentration in unburned foliage in ppm, $density_{fuel}$ is the fuel density of each biome in Mg/ha,[67] and $area_{burned}$ is the annual area of each biome subject to biomass burning in Mha.[68] This calculation was repeated for each biome and summed. The end result is an estimate of the total amount of Fe released due to burning foliage.

To account for uncertainties in $Fe_{aerosol}$ and $Fe_{foliage}$, two different methods were used to determine the annual flux of Fe from biomass burning aerosols: 1) weighted average, and 2) maximum value. In both methods, outliers in each foliage type were excluded using a Q test ($p < 0.05$). *P. ponderosa* Sample 3 and *P. aquatica* are outliers in unburned pine and tropical foliage, respectively. *B. gracilis* is an outlier in the percent of Fe aerosolized by burning grass herbage.

Method 1: Weighted Average (Table 2) The weighted averages for the percent Fe released from burning pine and eucalyptus foliage are negative because the concentration of Fe in the average field blanks for these burn sessions were larger than the amount of Fe collected during the experiment for these foliage types. In these calculations, negative percentages translate to these types of foliage are removing Fe, which is not physically possible. To account for this impossibility, these values were set to zero, and thus, boreal and arid tropical biomes have no calculated impact on the annual flux of Fe. Humid tropical and grassland/cropland biomes account for a flux of 27 ± 13 Gg of Fe per year.

Table 2: Global estimate of the Fe flux from burning foliage using Method 1.

Biome	Average Aerosolized Fe (%)	[Fe] in Foliage (ppm)	Fuel Density (Mg/ha)[67]	Burned Area (Mha/yr)[68]	Annual Fe Flux (Gg/yr)
Boreal forest	0 ± 0.01	49 ± 2	215 ± 73	8.7	0 ± 0
Tropical forest	0.37 ± 0.09	32 ± 3	220 ± 101	6	16 ± 8
Savannah and shrub	0 ± 0.04	19 ± 8	16 ± 11	350.2	0 ± 0
Grassland	0.06 ± 0.02	249 ± 35	7 ± 11	48.1	5 ± 7
Croplands	0.06 ± 0.02	249 ± 35	10 ± 9	46.9	7 ± 6
Total	**---**	**---**	**---**	**---**	**27 ± 13**

Method 2: Maximum values (Table 3) Using the maxima for the percent of Fe aerosolized and the Fe concentration of unburned foliage, the flux of Fe from burning foliage using this method is 114 ± 57 Gg Fe/yr. This figure represents an upper bound of Fe released from burning foliage.

Biome	Maximum Aerosolized Fe (%)	[Fe] in Foliage (ppm)	Fuel Density (Mg/ha)[67]	Burned Area (Mha/yr)[68]	Annual Fe Flux (Gg/yr)
Boreal forest	0.01 ± 0.09	58 ± 3	215 ± 73	8.7	0.9 ± 0.3
Tropical forest	0.8 ± 0.3	49 ± 3	220 ± 101	6	54 ± 31
Savannah and shrub	0.02 ± 0.04	113 ± 6	16 ± 11	350.2	12 ± 8
Grassland	0.128 ± 0.006	460 ± 23	7 ± 11	48.1	19 ± 30
Croplands	0.128 ± 0.006	460 ± 23	10 ± 9	46.9	29 ± 24
Total	---	---	---	---	**114 ± 57**

Table 3: Global estimate of the Fe flux from burning foliage using Method 2.

These estimates of the amount of Fe released from burning foliage are premised on several assumptions. First, that the foliage samples analyzed are accurate representations of the given biomes. Because biomes include many different types of plant, burning individual samples of each species may not be representative of the whole biome. Second, that the species collected are similar enough that an average may be taken. The amount of Fe in different species of plant may vary based on their metabolic needs; this would alter the range of Fe for plants in that biome.[23] Third, that the Fe concentration of collected samples and wild foliage are the same. These values may differ because the samples collected were typically grown in optimal growing conditions (water, sunlight, nutrients), but areas subject to burning may have water- or nutrient-

depleted soils that alter the amount of Fe that the plants can harvest.[69] In these instances, the concentration of Fe in the foliage may be smaller than measured.

With these assumptions in mind, these conservative estimates of the annual flux of Fe from burning foliage may be compared to values reported by recent studies. A recent modeling study suggests that the annual flux of Fe from biomass burning aerosols is 690 Gg/year, which includes both burning foliage aerosols and lofted soil particles.[17] Based on these estimates, burning foliage may account for up to 16% of the Fe from biomass burning aerosols. This result implies that the majority of the Fe from biomass burning aerosols is derived from lofted soil, which is consistent with the findings of previous studies.[14,31,55]

This result also implies that the Fe in biomass burning aerosols should have similar chemical characteristics to mineral dust sources. However, the smaller particle size created by biomass combustion lends itself to long atmospheric residence times and increased atmospheric processing. Biomass burning also creates acidic gases that could increase the solubility of these particles. As a result, we predict biomass burning aerosols to have increased solubility compared to mineral dust.

In summary, less than 2% of the Fe in foliage is released during biomass burning events. Extrapolated to a global scale, these results imply that during biomass burning events, at most 114 Gg of Fe in biomass burning aerosols is derived from burning foliage, which represents approximately 17% of the global flux of Fe from biomass burning events. The remaining 576 Gg of Fe is hypothesized to be derived from burning duff and soil entrainment. However, biomass burning aerosols may be more soluble than mineral dust due to long residence times and atmospheric processing by acidic gases. Future

studies should explore the composition of aerosols from burning duff, as well as the resulting particles' interactions with atmospheric gases over various time periods. With the anticipated increase in biomass burning events in coming years due to climate change,[70] the importance of biomass burning aerosols to the flux of Fe to the surface ocean may increase, thus potentially increasing marine primary productivity and altering the global carbon cycle.

CHAPTER 3

IMPLICATIONS

The results of my burn experiments indicate that burning duff and lofted soil particles provide most of the Fe in biomass burning aerosols. The following sections focus on the implications of my results in the context of 1) Fe isotopes, 2) soil impacts, 3) Fe solubility, 4) annual Fe flux, and 5) method improvements.

3.1 FE ISOTOPES

Mead and others[22] observed a non-dust source of fine particles that were isotopically distinct from mineral dust. They suggested these particles could have originated from biomass burning. In further research on Fe in fine aerosols Kurisu and others[29,71] measured Fe isotopes in anthropogenic aerosols and found the values were significantly lighter than in mineral dust. They attribute this fractionation to $FeCl_3$ evaporation during high temperature combustion (> 1000 ˚C). When $FeCl_3$ evaporates, light isotopes are preferentially taken into the gas phase before the heavier isotopes. Therefore, the Fe in aerosols generated from high-temperature combustion are very isotopically light compared to mineral dust. Biomass burning events, on the other hand, may only reach 800 ˚C, and thus $FeCl_3$ is unlikely to evaporate and fractionate Fe isotopes as significantly. Thus, isotope ratios observed in biomass burning aerosols may not be as light as the Fe isotope ratios observed in anthropogenic combustion aerosols.

The burn experiments conducted in Chapter 2 demonstrate that most of the Fe in biomass burning aerosols is derived from burning duff and lofted soil. This means that the Fe isotope composition of biomass burning aerosols may not be distinguishable from mineral dust sources. Kurisu and Takahashi[14] measured the Fe isotope composition of

biomass burning aerosols from a reed fire in Japan and concluded that Fe isotope ratios could not be used to distinguish biomass burning aerosols from mineral dust aerosols.

However, their measurements may only be relevant to biomass burning events that primarily involve grass herbage. Grasses and non-grass plants have developed distinct mechanisms for obtaining Fe from the soil, as much of the Fe in soil is in the insoluble Fe(III) oxidation state. Grasses take up Fe by releasing siderophores, large organic ligands, into the rhizosphere.[72] Organic complexation of Fe generally does not cause significant fractionation, therefore the Fe isotope ratios of soil and grass herbage should be similar.[26] However, other higher plants reduce Fe(III) to Fe(II) at their roots, which may induce a significant isotope fractionation.[73] Direct studies of Fe isotope ratios in plants by Guelke and von Blanckenberg[26] found that compared to the soil, grasses are isotopically unfractionated, whereas non-grasses show a distinct isotope fractionation.

The Fe isotopes in biomass burning aerosols could be a mixture of burned foliage and mineral dust. Aerosols derived from burning non-grass foliage could have a lighter Fe isotope composition than the surrounding soil, which would cause biomass burning aerosols to be slightly lighter overall than mineral dust. Therefore, there may be a slight Fe isotope variation between biomass burning aerosols and mineral dust if a significant amount of non-grass plant material was burned. However, more studies on Fe isotopes in biomass burning aerosols of non-grassy plants versus grassy plants are needed to fully settle this question. In addition, the Fe released by burning duff should be directly measured as well to determine if the Fe isotopes in these aerosols resembles mineral dust.

3.2 IMPACT OF SOIL

The amount of Fe in biomass burning aerosols could be controlled by the Fe availability of the surrounding soil. In this study, I examined the Fe content of several types of foliage, and I observed that grass samples had a significantly higher Fe concentration than the Fe in the other foliage samples. I also observed that burning these grass samples produced aerosols with a higher Fe content than the other types of foliage. I attribute this to the basaltic soil in which these samples grew. Basaltic soils weather easily, releasing Fe into the surrounding soils. Plants increase their uptake of Fe when they are planted in Fe-rich soil. While there are limits due to the damage that Fe can induce to plant cells through the Fenton reaction, soil Fe content directly impacts the amount of Fe in associated plant matter.

Therefore, the amount of available Fe in the soil may control the amount of Fe released by a biomass burning event. For example, a forest fire occurring in an area with basaltic soil would generate biomass burning aerosols with a higher Fe content than a forest fire occurring in an area with non-basaltic soils. To explore this idea, future studies should compare the Fe in atmospheric particles collected over various regions around the world to geologic maps indicating the presence of basaltic rocks. These studies should aim to determine if biomass burning aerosols generated from areas with basaltic-derived soils have a higher Fe content than biomass burning aerosols from non-basaltic areas.

3.3 FE SOLUBILITY

Based on my estimates of the Fe flux from burning foliage and the solubility of mineral dust, biomass burning, and anthropogenic aerosols,[17] it is possible to derive an approximate amount of soluble Fe from biomass burning activities. Biomass burning

aerosols have an Fe solubility of 21%. If we assume uniform Fe solubility in all biomass burning aerosols (i.e., that aerosols derived from burning foliage are not more soluble than entrained soil or aerosols derived from burning duff), then the maximum amount of soluble Fe from burning foliage is approximately 23 Gg of Fe per year.

However, the solubility of biomass burning particles may decrease with increasing percent composition of mineral dust, as mineral dust has a very low solubility. If this is the case, and the solubility of Fe in aerosols from burning foliage more closely resembles the solubility of anthropogenic aerosols (at 65% solubility), this figure increases to approximately 74.1 Gg of Fe per year, which would represent about half of the total flux of soluble Fe from biomass burning aerosols.

It is possible to determine the burned foliage-to-entrained soil ratio by assuming that biomass burning aerosols are a mixture of anthropogenic combustion-like particles and mineral dust particles. The solubility of biomass burning aerosols (21%) falls between anthropogenic combustion aerosols (65%) and mineral dust (2%). If burning foliage has a solubility resembling anthropogenic aerosols, and entrained soil has a solubility resembling mineral dust, a mixing model may enable an estimate the amount of Fe from each source contained within biomass burning aerosols. Using mineral dust and anthropogenic aerosols as two end members, I determine that approximately 30% of the soluble Fe in biomass burning aerosols is derived from burning foliage.

This figure is nearly twice my estimate of the contribution of burning foliage (17%). There are a few explanations for this discrepancy. First, our experiments measured the amount of Fe in unprocessed aerosols. Processing of suspended soil by acidic gases generated from biomass burning would increase their solubility, which

would decrease the percentage of Fe coming from foliage. For example, if atmospheric processing raises dust solubility to 10%, the overall contribution of foliage to biomass burning aerosols decreases to 20%, which is much closer to my estimate. More research is needed into how the solubility of mineral dust aerosols changes as they are processed.

3.4 ANNUAL FE FLUX

Globally, mineral dust contributes the most soluble Fe to atmospheric aerosols. Mineral dust contributes 1580 Gg of soluble Fe annually, compared to anthropogenic combustion and biomass burning at 462 and 145 Gg per year of Fe, respectively.[17] This study strengthens the importance of mineral dust, as I estimate that approximately 83% of the Fe in biomass burning aerosols is derived from entrained soil particles.

Regionally, however, biomass burning may significantly impact the Fe flux to HNLC areas, such as the Southern Ocean. A modeling study by Ito suggests that in the southern hemisphere, biomass burning aerosols may contribute up to 60% of the soluble Fe deposited on surface waters.[17] This is particularly critical in the Southern Ocean, one of the largest HNLC areas on the planet. The location in which these aerosols are deposited is as important as the amount of Fe deposited from each aerosol source. Further studies are needed to confirm this modeling observation. Such studies would measure the Fe content in aerosols in the Southern Ocean and Equatorial Pacific, and, using Fe isotopes, soluble potassium, or other tracers for biomass burning, determine the percentage of Fe in these marine aerosols that is derived from biomass burning events.

3.5 METHOD IMPROVEMENTS

For future experiments, several methodological changes would improve the quality of these experiments. First, burning replicates of each type of material would

improve the error estimated mass fluxes produced in this study. Second, a quantitative method to collect ash samples would allow closure of the mass balance among unburned foliage, aerosols, and ash. Third, burning duff and leaf litter in addition to foliage would directly test the hypothesis that biomass burning aerosols are primarily derived from soil. Fourth, burning a larger mass of material would collect more Fe. Significant modifications would have to be made to the experimental setup to accomplish this, such as utilizing longer ductwork and/or designing a better system for particle collection than the cellulose filters. Finally, the most significant improvement would be to conduct the experiment in an enclosed, slightly pressurized space with HEPA-filtered air. These experiments were conducted outside, which led to large field blank values compared to collected burn aerosol values. Conducting these experiments in an enclosed area free from the impact of mineral dust would drastically improve these measurements.

REFERENCES

(1) Falkowski, P. G., Barber, R. T., and Smetacek, V. (1998) Biogeochemical controls and feedbacks on ocean primary production. *Science 281*, 200–206.

(2) Mahowald, N. M., Baker, A. R., Bergametti, G., Brooks, N., Duce, R. A., Jickells, T. D., Kubilay, N., Prospero, J. M., and Tegen, I. (2005) Atmospheric global dust cycle and iron inputs to the ocean. *Global Biogeochem. Cycles 19*, GB4025.

(3) Balk, J., and Schaedler, T. A. (2014) Iron Cofactor Assembly in Plants. *Annu. Rev. Plant Biol. 65*, 125–153.

(4) Wu, B., Amelung, W., Xing, Y., Bol, R., and Berns, A. E. (2019) Iron cycling and isotope fractionation in terrestrial ecosystems. *Earth-Science Rev. 190*, 323–352.

(5) Tagliabue, A., Sallée, J.-B., Bowie, A. R., Lévy, M., Swart, S., and Boyd, P. W. (2014) Surface-water iron supplies in the Southern Ocean sustained by deep winter mixing. *Nat. Geosci. 7*, 314–320.

(6) Homoky, W. B., John, S. G., Conway, T. M., and Mills, R. a. (2013) Distinct iron isotopic signatures and supply from marine sediment dissolution. *Nat. Commun. 4*, 2143.

(7) Conway, T. M., and John, S. G. (2014) Quantification of dissolved iron sources to the North Atlantic Ocean. *Nature 511*, 212–215.

(8) Lam, P. J., and Bishop, J. K. B. (2008) The continental margin is a key source of iron to the HNLC North Pacific Ocean. *Geophys. Res. Lett. 35*, 1–5.

(9) Duce, R. A., and Tindale, N. W. (1991) Chemistry and biology of iron and other trace metals in the ocean. *Limnol. Oceanogr. 36*, 1715–1726.

(10) Jickells, T. D. (2005) Global Iron Connections Between Desert Dust, Ocean Biogeochemistry, and Climate. *Science 308*, 67–71.

(11) Luo, C., Mahowald, N., Bond, T., Chuang, P. Y., Artaxo, P., Siefert, R., and Chen, Y. (2008) Combustion iron distribution and deposition. *Global Biogeochem. Cycles 22*, 1–17.

(12) Paris, R., Desboeufs, K. V., Formenti, P., Nava, S., and Chou, C. (2010) Chemical characterisation of iron in dust and biomass burning aerosols during AMMA-SOP0/DABEX: Implication for iron solubility. *Atmos. Chem. Phys. 10*, 4273–4282.

(13) Ito, A. (2015) Atmospheric processing of combustion aerosols as a source of bioavailable iron. *Environ. Sci. Technol. Lett. 2*, 70–75.

(14) Kurisu, M., and Takahashi, Y. (2019) Testing Iron Stable Isotope Ratios as a Signature of Biomass Burning. *Atmosphere 10*, 76.

(15) Baker, A. R., and Jickells, T. D. (2006) Mineral particle size as a control on aerosol iron solubility. *Geophys. Res. Lett. 33*, 1–4.

(16) De Jong, J. T. M., Den Das, J., Bathmann, U., Stoll, M. H. C., Kattner, G., Nolting, R. F., and De Baar, H. J. W. (1998) Dissolved iron at subnanomolar levels in the Southern Ocean as determined by ship-board analysis. *Anal. Chim. Acta 377*, 113–124.

(17) Ito, A. (2015) Atmospheric Processing of Combustion Aerosols as a Source of Bioavailable Iron. *Environ. Sci. Technol. Lett. 2*, 70–75.

(18) Andreae, M. O. (1983) Soot Carbon and Excess Fine Potassium: Long-Range Transport of Combustion-Derived Aerosols. *Science 220*, 1148–1151.

(19) Fraser, M. P., and Lakshmanan, K. (2000) Using levoglucosan as a molecular marker for the long-range transport of biomass combustion aerosols. *Environ. Sci. Technol. 34*, 4560–4564.

(20) Hennigan, C. J., Sullivan, A. P., Collett, J. L., and Robinson, A. L. (2010) Levoglucosan stability in biomass burning particles exposed to hydroxyl radicals. *Geophys. Res. Lett. 37*, 2–5.

(21) Urey, H. C. (1947) The Thermodynamic Properties of Isotopic Substances. *J. Chem. Soc.* 562–581.

(22) Mead, C., Herckes, P., Majestic, B. J., and Anbar, A. D. (2013) Source apportionment of aerosol iron in the marine environment using iron isotope analysis. *Geophys. Res. Lett. 40*, 5722–5727.

(23) von Blanckenburg, F., von Wiren, N., Guelke, M., Weiss, D. J., and Bullen, T. D. (2009) Fractionation of metal stable isotopes by higher plants. *Elements 5*, 375–380.

(24) Guelke, M., von Blanckenburg, F., Schoenberg, R., Staubwasser, M., and Stuetzel, H. (2010) Determining the stable Fe isotope signature of plant-available iron in soils. *Chem. Geol. 277*, 269–280.

(25) Guelke-Stelling, M., and von Blanckenburg, F. (2012) Fe isotope fractionation caused by translocation of iron during growth of bean and oat as models of strategy I and II plants. *Plant Soil 352*, 217–231.

(26) Guelke, M., and von Blanckenburg, F. (2007) Fractionation of Stable Iron Isotopes in Higher Plants. *Environ. Sci. Technol. 41*, 1896–1901.

(27) Kurisu, M., Sakata, K., Miyamoto, C., Takaku, Y., Iizuka, T., and Takahashi, Y. (2016) Variation of Iron Isotope Ratios in Anthropogenic Materials Emitted through Combustion Processes. *Chem. Lett. 45*, 970–972.

(28) Kurisu, M., Takahashi, Y., Iizuka, T., and Uematsu, M. (2016) Very low isotope

ratio of iron in fine aerosols related to its contribution to the surface ocean. *J. Geophys. Res. Atmos. 121*, 119–136.

(29) Kurisu, M., Adachi, K., Sakata, K., and Takahashi, Y. (2019) Stable Isotope Ratios of Combustion Iron Produced by Evaporation in a Steel Plant. *ACS Earth Sp. Chem. 3*, 588-598.

(30) Majestic, B. J., Anbar, A. D., and Herckes, P. (2009) Elemental and iron isotopic composition of aerosols collected in a parking structure. *Sci. Total Environ. 407*, 5104–5109.

(31) Guieu, C., Bonnet, S., Wagener, T., and Loÿe-Pilot, M. D. (2005) Biomass burning as a source of dissolved iron to the open ocean? *Geophys. Res. Lett. 32*, 1–5.

(32) Yamasoe, M. A., Artaxo, P., Miguel, A. H., and Allen, A. G. (2000) Chemical composition of aerosol particles from direct emissions of vegetation fires in the Amazon Basin: Water-soluble species and trace elements. *Atmos. Environ. 34*, 1641–1653.

(33) Christian, T. J., Kleiss, B., Yokelson, R. J., Holzinger, R., Crutzen, P. J., Hao, W. M., Saharjo, B. H., Ward, D., and E. (2003) Comprehensive laboratory measurements of biomass-burning emissions: 1. Emissions from Indonesian, African, and other fuels. *J. Geophys. Res. 108*, 4719.

(34) Burling, I. R., Yokelson, R. J., Griffith, D. W. T., Johnson, T. J., Veres, P., Roberts, J. M., Warneke, C., Urbanski, S. P., Reardon, J., Weise, D. R., Hao, W. M., and de Gouw, J. (2010) Laboratory measurements of trace gas emissions from biomass burning of fuel types from the southeastern and southwestern United States. *Atmos. Chem. Phys. 10*, 11115–11130.

(35) Martin, J. H. (1989) Glacial-Interglacial CO2 Change: The Iron Hypothesis. *Paleoceanography 5*, 1–13.

(36) Gledhill, M., and Buck, K. N. (2012) The organic complexation of iron in the marine environment: A review. *Front. Microbiol. 3*, 1–17.

(37) Moore, C. M., Mills, M. M., Arrigo, K. R., Berman-Frank, I., Bopp, L., Boyd, P. W., Galbraith, E. D., Geider, R. J., Guieu, C., Jaccard, S. L., Jickells, T. D., La Roche, J., Lenton, T. M., Mahowald, N. M., Maranon, E., Marinov, I., Moore, J. K., Nakatsuka, T., Oschlies, A., Saito, M. A., Thingstad, T. F., Tsuda, A., and Ulloa, O. (2013) Processes and patterns of oceanic nutrient limitation. *Nat. Geosci 6*, 701–710.

(38) Boyd, P. W., and Ellwood, M. J. (2010) The biogeochemical cycle of iron in the ocean. *Nat. Geosci. 3*, 675–682.

(39) Martin, J. H., Coale, K. H., Johnson, K. S., Fitzwater, S. E., Gordon, R. ., Tanner, S. J., Hunter, C. N., Elrod, V. A., Nowicki, J. L., Coley, T. ., Barber, R. T., Lindley, S., Watson, A. J., Van Scoy, K., Law, C. ., Liddicoat, M. I., Ling, R., Stanton, T., Stockel, J.,

Collins, C., Anderson, A., Bidigare, R., Ondrusek, M., Latasa, M., Millero, F. ., Lee, K., Yao, W., Zhang, J. Z., Friedrich, G., Sakamoto, C., Chavez, F., Buck, K., Kolber, Z., Greene, R., Falkowski, P., Chisholm, S. W., Hoge, F., Swift, R., Yungel, J., Turner, S., Nightingale, P., Hatton, A., Liss, P., and TIndale, N. W. (1994) Testing the iron hypothesis in ecosystems of the equatorial Pacific Ocean. *Nature 371*, 123–129.

(40) Fung, I. Y., Meyn, S. K., Tegen, I., Doney, S. C., John, J. G., and Bishop, J. K. B. (2000) Iron supply and demand in the upper ocean. *Global Biogeochem. Cycles 14*, 281–295.

(41) Hooper, J., Mayewski, P., Marx, S., Henson, S., Potocki, M., Sneed, S., Handley, M., Gassó, S., Fischer, M., and Saunders, K. M. (2018) Examining links between dust deposition and phytoplankton response using ice cores. *Aeolian Res. 36*, 45–60.

(42) Chu, N. C., Johnson, C. M., Beard, B. L., German, C. R., Nesbitt, R. W., Frank, M., Bohn, M., Kubik, P. W., Usui, A., and Graham, I. (2006) Evidence for hydrothermal venting in Fe isotope compositions of the deep Pacific Ocean through time. *Earth Planet. Sci. Lett. 245*, 202–217.

(43) Resing, J. A., Sedwick, P. N., German, C. R., Jenkins, W. J., Moffett, J. W., Sohst, B. M., and Tagliabue, A. (2015) Basin-scale transport of hydrothermal dissolved metals across the South Pacific Ocean. *Nature 523*, 200–203.

(44) Bopp, L., Tagliabue, A., Remenyi, T., Bucciarelli, E., Jeandel, C., Jean-Baptiste, P., Bowie, A. R., Aumont, O., Gehlen, M., Lannuzel, D., Dutay, J.-C., Sarthou, G., and Chever, F. (2010) Hydrothermal contribution to the oceanic dissolved iron inventory. *Nat. Geosci. 3*, 252–256.

(45) Tagliabue, A., and Resing, J. A. (2016) Impact of hydrothermalism on the ocean iron cycle. *Philos. Trans. A 374*, in Press.

(46) John, S. G., Mendez, J., Moffett, J., and Adkins, J. (2012) The flux of iron and iron isotopes from San Pedro Basin sediments. *Geochim. Cosmochim. Acta 93*, 14–29.

(47) Homoky, W. B., Weber, T., Berelson, W. M., Conway, T. M., Henderson, G. M., van Hulten, M., Jeandel, C., Severmann, S., and Tagliabue, A. (2016) Quantifying trace element and isotope fluxes at the ocean–sediment boundary: a review. *Philos. Trans. R. Soc. A Math. Phys. Eng. Sci. 374*, 20160246.

(48) Buck, C. S., Aguilar-Islas, A., Marsay, C., Kadko, D., and Landing, W. M. (2019) Trace element concentrations, elemental ratios, and enrichment factors observed in aerosol samples collected during the US GEOTRACES eastern Pacific Ocean transect (GP16). *Chem. Geol.* 0–1.

(49) Schroth, A. W., Crusius, J., Sholkovitz, E. R., and Bostick, B. C. (2009) Iron solubility driven by speciation in dust sources to the ocean. *Nat. Geosci. 2*, 337–340.

(50) Sedwick, P. N., Sholkovitz, E. R., and Church, T. M. (2007) Impact of anthropogenic combustion emissions on the fractional solubility of aerosol iron: Evidence from the Sargasso Sea. *Geochemistry, Geophys. Geosystems 8*.

(51) Ito, A., and Xu, L. (2014) Response of acid mobilization of iron-containing mineral dust to improvement of air quality projected in the future. *Atmos. Chem. Phys. 14*, 3441–3459.

(52) Scanza, R. A., Hamilton, D. S., Perez Garcia-Pando, C., Buck, C., Baker, A., and Mahowald, N. M. (2018) Atmospheric processing of iron in mineral and combustion aerosols: development of an intermediate-complexity mechanism suitable for Earth system models. *Atmos. Chem. Phys. 18*, 14175–14196.

(53) Meskhidze, N. (2003) Iron mobilization in mineral dust: Can anthropogenic SO 2 emissions affect ocean productivity? . *Geophys. Res. Lett. 30*, 1–5.

(54) Liu, X., Fu, P., Shi, Z., Zhang, X., Zhang, J., Nenes, A., Wang, W., Shao, L., Harrison, R. M., Yao, X., Li, W., Xu, L., Chen, J., Zhang, D., Lin, Y., and Gao, H. (2017) Air pollution–aerosol interactions produce more bioavailable iron for ocean ecosystems. *Sci. Adv. 3*, e1601749.

(55) Gaudichet, A., Echalar, F., Chatenet, B., Quisefit, J. P., and Malingre, G. (1995) Trace Elements in Tropical African Savanna Biomass Burning Aerosols. *J. Atmos. Chem. 22*, 19–39.

(56) Yokelson, R. J., Griffith, D. W. T., and Ward, D. E. (1996) Open-path Fourier transform infrared studies of large-scale laboratory biomass fires. *J. Geophys. Res. Atmos. 101*, 21067–21080.

(57) Howard, A. G., and Statham, P. J. (1993) Inorganic Trace Analysis: Philosophy and Practice. Wiley, Chichester, New York.

(58) Oliva, S. R., and Raitio, H. (2003) Review of cleaning techniques and their effects on the chemical composition of foliar samples. *Boreal Environ. Res. 8*, 263–272.

(59) Hosseini, S., Urbanski, S. P., Dixit, P., Qi, L., Burling, I. R., Yokelson, R. J., Johnson, T. J., Shrivastava, M., Jung, H. S., Weise, D. R., Miller, J. W., and Cocker, D. R. (2013) Laboratory characterization of PM emissions from combustion of wildland biomass fuels. *J. Geophys. Res. Atmos. 118*, 9914–9929.

(60) Upadhyay, N., Majestic, B. J., Prapaipong, P., and Herckes, P. (2009) Evaluation of polyurethane foam, polypropylene, quartz fiber, and cellulose substrates for multi-element analysis of atmospheric particulate matter by ICP-MS. *Anal. Bioanal. Chem. 394*, 255–266.

(61) Hagen-Thorn, A., and Stjernquist, I. (2005) Micronutrient levels in some temperate European tree species: A comparative field study. *Trees - Struct. Funct. 19*, 572–579.

(62) Reimann, C., Fabian, K., Flem, B., Andersson, M., Filzmoser, P., and Englmaier, P. (2018) Geosphere-biosphere circulation of chemical elements in soil and plant systems from a 100 km transect from southern central Norway. *Sci. Total Environ. 639*, 129–145.

(63) Schlegel, P., Wyss, U., Arrigo, Y., and Hess, H. D. (2016) Mineral concentrations of fresh herbage from mixed grassland as influenced by botanical composition, harvest time and growth stage. *Anim. Feed Sci. Technol. 219*, 226–233.

(64) Aiuppa, A., Allard, P., D'Alessandro, W., Michel, A., Parello, F., Treuil, M., and Valenza, M. (2000) Mobility and fluxes of major, minor and trace metals during basalt weathering and groundwater transport at Mt. Etna volcano (Sicily). *Geochim. Cosmochim. Acta 64*, 1827–1841.

(65) Burghelea, C., Zaharescu, D. G., Dontsova, K., Maier, R., Huxman, T., and Chorover, J. (2015) Mineral nutrient mobilization by plants from rock: influence of rock type and arbuscular mycorrhiza. *Biogeochemistry 124*, 187–203.

(66) Duce, R. A., and Tindale, N. W. (1991) Chemistry and Biology of Iron and Other Trace Metals. *Limnol. Ocanography 36*, 1715–1726.

(67) Pettinari, M. L., and Chuvieco, E. (2016) Generation of a global fuel data set using the Fuel Characteristic Classification System. *Biogeosciences 13*, 2061–2076.

(68) Randerson, J. T., Chen, Y., Van Der Werf, G. R., Rogers, B. M., and Morton, D. C. (2012) Global burned area and biomass burning emissions from small fires. *J. Geophys. Res. G Biogeosciences 117*.

(69) Cai, J., Weiner, J., Wang, R., Luo, W., Zhang, Y., Liu, H., Xu, Z., Li, H., Zhang, Y., and Jiang, Y. (2017) Effects of nitrogen and water addition on trace element stoichiometry in five grassland species. *J. Plant Res. 130*, 659–668.

(70) Huang, Y., Wu, S., and Kaplan, J. O. (2014) Sensitivity of global wildfire occurrences to various factors in thecontext of global change. *Atmos. Environ. 121*, 86–92.

(71) Kurisu, M., Sakata, K., Miyamoto, C., Takaku, Y., Iizuka, T., and Takahashi, Y. (2016) Variation of Iron Isotope Ratios in Anthropogenic Materials Emitted through Combustion Processes. *Chem. Lett. 45*, 970–972.

(72) Marschner, H., Romheld, V. (1994) Strategies of plants for acquisition of iron. *Plant Soil 165*, 261–274.

(73) Anbar, A. D., Jarzecki, A. A., and Spiro, T. G. (2005) Theoretical investigation of iron isotope fractionation between Fe(H2O)63+ and Fe(H2O)62+: Implications for iron stable isotope geochemistry. *Geochim. Cosmochim. Acta 69*, 825–837.

APPENDIX A

PROTOCOL: CELLULOSE FILTER CLEANING

Note: Always wear gloves and tweezers when handling filters.

1) Remove cellulose filters (full or slotted) from package individually and place on plastic mesh
2) Rinse with 18 MΩ-cm DI water and place in labelled plastic container
3) Repeat for as many filters as needed (container holds about 20 filters), placing them on top of each other.
4) Rinse each filter twice more, working through the pile of filters.
5) Place all filters into the container.
6) Add reagent-grade conc HCl (2% solution, 2 L) to the container.
7) Leave overnight
8) Empty container of acid into waste
9) Rinse each filter at least three times using 18 MΩ-cm DI water
10) Repeat Steps 5-9 for a total of three cleaning cycles.
11) Let filters dry in plastics hood.
12) When dry, place each filter into individual zipper bags (gallon for 203x241 mm filters, quart for slotted filters). Label each bag with the date that the filters were placed into the bag.

APPENDIX B

PROTOCOL: MICROWAVE DIGESTION

These instructions are for the CEM Discover located in PSF 066.

Note: During digesting, reflux concentrated HCl (approx. half the volume of the beaker) in all post-digestion Teflon beakers.

1) Pre-Digestion Procedure (use Class 10 Laminar Flow hood)
    a) Make sure that enough vessels are clean, including glass, caps, stir bars, and (if HF is used) Teflon liners.
    b) Assemble the vessels:
        i) Place a Teflon liner in the glass vessel (especially with HF) and add a stir bar using tweezers
    c) Carefully add samples to the vessels using weigh paper or a weigh boat.
    d) Add digestion reagents.
        i) Clean foliage: 10 mL HNO_3
        ii) Burn aerosols: 10 mL conc. HNO_3, 4 mL DI H_2O, and 1 mL conc. HF.
        iii) Ash: 10 mL HNO_3
    e) Cap samples before transport
2) Digester Setup
    a) Make sure the outlet vent in the adjacent hood is uncapped.
    b) Turn on the air (valve on the wall) and the fan (switch on the autosampler near the bubbler).
    c) Wear gloves to place samples into the autosampler.
        i) Any marker labels will wear off in the digestion process. Sketch a simple diagram of vessels to keep track of samples.
    d) If HF is used, add 1g of boric acid to the bubbler for every 1 mL of HF.

(1) Add ~75% of the boric acid to initial bubbler. Add the rest to the second bubbler. Stir the resulting solutions.

e) On the computer:

i) In the Data/Methods window, select your method.

(1) In the diagram of the sample racks, click on the positions of each sample, right-click on the position, and select "Add Method."

(a) For unburned foliage, use "Biomass" method for first round of digestions, "BBA Soot" for second round

(b) For aerosols, use "BBA" method

(c) For ash, use "BBA Soot" method

f) Run a "Water Clean" method at the end to flush out the system.

i) Fill a digestion vessel with approximately the same volume of tap water as acid in the samples.

ii) Add the "Water Clean" method to the end of the queue.

g) Press the green Play button at the top of the window to begin digesting

3) Post-Digestion Procedure

a) Wear gloves and carefully remove samples from the autosampler.

b) Place the glass vials into the magnetic cup to keep the stir bar in the vial Carefully pour samples into the "post-digestion" beakers, rotating the vessel each time to remove any adhered sample.

i) Set aside vessels if a second round of digestion is needed. Clean all vessels when digestion is completed.

c) Transfer to one of the dry-down hoods, uncap the beakers and place them onto a hot plate, leaving at least 0.5 cm of space between each sample.
    i) Place a Post-It on the plastic door with your name, the date, and contents.
    ii) Reduce volume to near dryness.
    iii) Add 5 mL of conc HNO_3 to each beaker and transfer back to glass vial. Repeat for a total of 10 mL conc HNO_3. Add additional reagents if applicable.

4) Vessel cleaning procedure
    a) Add the same volume of reagents used to digest samples.
    b) Cap each vessel with a new cap.
        i) Caps last through two digestion cycles. Using new caps with these vessels ensures that the caps are clean.
    c) Digest the samples using the same method used to digest samples.
    d) After completing the digestion, place vessels into magnetic cup and discard the solution in a waste container.
    e) Remove the stir bars after discarding the cleaning solution. Place them into a small, clean Teflon beaker
    f) Rinse all components with 18MΩ H_2O at least 5x.
    g) Place them in the Low-Fe hood to air dry.
    h) When dry, reassemble the vessels and cap

Ramp Procedures:

1. Unburned Foliage
    a. Microwave: CEM DISCOVER
    b. Method: BIOMASS
        i. Ramp to 220 ˚C and 225 psi over 20 minutes
        ii. Hold for 10 minutes
        iii. Cool for 5-10 minutes (or until temperature fell below 60 ˚C)
2. Cellulose filters and ash
    a. Microwave: CEM MARS5
    b. Method: AIRPUFF PP (per Upadhyay et al. 2009)[60]
        i. Ramp to 140 ˚C for 3 minutes
        ii. Hold for 3 minutes
        iii. Ramp to 160 ˚C for 3 minutes
        iv. Hold for 3 minutes
        v. Ramp to 180 ˚C for 3 minutes
        vi. Hold for 15 minutes
        vii. Cool for at least 1 hour

APPENDIX C

PROTOCOL: HOTPLATE DIGESTION

1) Nitric/Peroxide: to remove organics
    a) Time on hotplate: 2 hours
    b) Reagents: 750 µL conc HNO_3 + 250 µL concentrated H_2O_2
    c) Post-digestion: Sonicate for 5 min and dry samples to near dryness
2) Aqua Regia: to remove difficult organics
    a) Time on hotplate: Overnight
    b) Reagents: 3 mL concentrated HCl + 1 mL concentrated HNO_3
    c) Post-digestion: Sonicate for 5 min and dry samples to near dryness
3) Nitric/HF: To remove silicates
    a) Time on hotplate: Overnight
    b) Reagents: 4 mL concentrated HNO_3 + 1 mL concentrated HF
        i) USE CAUTION WHEN WORKING WITH HF
    c) Post-digestion: Sonicate for 5 min and dry samples to near dryness
4) Hydrochloric: To break down SiF_4 crystals that may form
    a) Time on hotplate: Overnight
    b) Reagents: 5 mL concentrated HCl
    c) Post-digestion: Sonicate for 5 min and dry samples to near dryness
    d) Repeat as needed
5) Nitric/peroxide
    a) Time on hotplate: 2 hours
    b) Reagents: 500 µL concentrated HNO_3 + 100 µL concentrated H_2O_2
    c) Post-digestion: Sonicate for 5 min and dry samples to near dryness
    d) Repeat as needed to dissolve any solids

APPENDIX D

DATA: FE IN ANALYZED SAMPLES

Table 4: Fe concentrations in field blank samples.

Field Blank	Fine ($\mu g\ filter^{-1}$)	Coarse ($\mu g\ filter^{-1}$)
1	3.4 (0.84)	19.12 (0.98)
2	9.22 (0.96)	1.81 (0.13)
3	11.86 (1.66)	2.57 (0.15)
4	5.08 (1.56)	1.32 (0.1)
5	3.52 (1.55)	0.79 (0.08)
6	1.9 (1.53)	0.78 (0.08)
7	1.22 (1.53)	0.16 (0.07)
8	19.56 (1.38)	7.33 (0.63)
9	2.91 (0.87)	1 (0.49)
10	2.29 (0.86)	0.88 (0.49)
11	5.61 (0.92)	2.14 (0.5)

Table 5: Fe in unburned foliage, ash, coarse, and fine samples. The Fe concentration of reagent blanks were subtracted from each sample. Average filter blanks were subtracted from coarse and fine filters.

Sample Name	Unburned Foliage (mg)	Ash (mg)	Fine (μg filter^{-1})	Coarse (μg filter^{-1})
Pinus ponderosa 1	6.3 (0.3)	6.8 (0.3)	3.87 (0.85)	0.59 (0.08)
Pinus ponderosa 2	7.6 (0.4)	12.1 (0.6)	5.66 (0.88)	21.13 (1.08)
Pinus ponderosa 3	8.4 (0.4)	8.3 (0.4)	6.16 (0.89)	9.69 (0.51)
Pinus ponderosa 4	7.9 (0.4)	9.7 (0.5)	5.53 (0.87)	2.22 (0.15)
Arenga pinnata	1.84 (0.09)	0.93 (0.05)	13.87 (1.71)	2.15 (0.13)
Bambusa spp.	1.07 (0.05)	0.98 (0.05)	10.97 (1.65)	1.58 (0.11)
Cissus sicyoides	0.69 (0.03)	0.183 (0.009)	14.4 (1.72)	2.94 (0.16)
Costas spp.	0.92 (0.05)	0.32 (0.02)	6.78 (1.58)	1.43 (0.1)
Elaeis guianensis	2.9 (0.1)	2.2 (0.1)	6.1 (1.57)	1.28 (0.1)
Inga spp.	1.19 (0.06)	2 (0.1)	5.9 (1.57)	0.45 (0.07)
Melia azedarach	2.3 (0.1)	2.1 (0.1)	4.01 (1.55)	1.52 (0.1)
Musa spp.	2 (0.1)	1.31 (0.07)	5.07 (1.56)	0.42 (0.07)
Pachira aquatica	3.9 (0.2)	7.2 (0.4)	25.9 (2.05)	1.01 (0.09)
Spathodea campanulata	1.13 (0.06)	1.23 (0.06)	3.1 (1.54)	1.02 (0.09)
Eucalyptus camaldulensis	11 (0.6)	8.1 (0.4)	1.97 (1.54)	4.01 (0.21)
Eucalyptus erythrocorys	6.6 (0.3)	**	11.35 (1.08)	2.63 (0.51)
Eucalyptus microtheca	6.2 (0.3)	10.9 (0.5)	4.62 (0.9)	0.44 (0.48)
Eucalyptus papuana	2.6 (0.1)	2 (0.1)	2.37 (0.86)	0.71 (0.48)
Eucalyptus woodwardii	0.016 (0.001)	0.73 (0.04)	4.73 (0.9)	1.2 (0.49)
Pascopyrum smithii	10.9 (0.5)	17 (0.8)	13.08 (1.13)	3.41 (0.52)
Elymus elymoides	24 (1)	28 (1)	37.02 (2.14)	8.86 (0.68)
Thinopyrum intermedium	5.7 (0.3)	6.3 (0.3)	9.78 (1.03)	5.27 (0.57)
Bouteloua gracilis	12.9 (0.6)	27 (1)	94.23 (4.91)	12.47 (0.82)
Sorghastrum nutans	12.4 (0.6)	17.2 (0.9)	21.63 (1.46)	5.41 (0.57)

**Sample was lost during processing.

APPENDIX E

DATA: TRACE METALS IN UNBURNED FOLIAGE

Table 6: Unburned foliage concentrations of Na, Mg, Al. P, K, Ca, Ti, and V. The reagent blank concentration of each trace metal analyzed was subtracted from the unburned foliage samples.

Sample Name	Na (mg)	Mg (mg)	Al (mg)	P (mg)	K (mg)	Ca (mg)	Ti (µg)	V (µg)
Pinus ponderosa 1	25 (1)	64 (3)	18.1 (0.9)	147 (7)	578 (29)	83 (4)	477 (24)	10.1 (0.5)
Pinus ponderosa 2	45 (2)	73 (4)	16 (0.8)	186 (9)	935 (47)	109 (5)	473 (24)	9 (0.4)
Pinus ponderosa 3	12.3 (0.6)	100 (5)	23 (1)	137 (7)	478 (24)	163 (8)	668 (33)	13 (0.6)
Pinus ponderosa 4	26 (1)	105 (5)	22 (1)	188 (9)	603 (30)	149 (7)	520 (26)	9.4 (0.5)
Arenga pinnata	16.3 (0.8)	85 (4)	0.44 (0.02)	61 (3)	257 (13)	483 (24)	29 (1)	5.5 (0.3)
Bambusa spp.	8.5 (0.4)	33 (2)	0.26 (0.01)	50 (3)	430 (22)	113 (6)	21 (1)	0.012 (0.001)
Cissus sicyoides	7 (0.3)	32 (2)	0.056 (0.003)	74 (4)	285 (14)	942 (47)	7.4 (0.4)	3 (0.1)
Costas spp.	10.9 (0.5)	64 (3)	0.4 (0.02)	37 (2)	500 (25)	362 (18)	28 (1)	0.86 (0.04)
Elaeis guianensis	30 (2)	168 (8)	0.48 (0.02)	74 (4)	617 (31)	698 (35)	40 (2)	1.7 (0.08)
Inga spp.	13.4 (0.7)	80 (4)	0.2 (0.01)	43 (2)	181 (9)	369 (18)	20 (1)	0.4 (0.02)
Melia azedarach	20 (1)	451 (23)	0.54 (0.03)	139 (7)	651 (33)	1019 (51)	31 (2)	1.06 (0.05)
Musa spp.	14.3 (0.7)	40 (2)	0.65 (0.03)	38 (2)	970 (48)	450 (23)	76 (4)	0.6 (0.03)
Pachira aquatica	11.8 (0.6)	60 (3)	0.68 (0.03)	38 (2)	274 (14)	404 (20)	251 (13)	0.75 (0.04)
Spathodea campanulata	5.3 (0.3)	59 (3)	0.19 (0.01)	50 (3)	312 (16)	268 (13)	14.1 (0.7)	0.31 (0.02)
Eucalyptus camaldulensis	86 (4)	361 (18)	15.8 (0.8)	121 (6)	413 (21)	2068 (103)	807 (40)	18 (0.9)
Eucalyptus erythrocorys	1043 (52)	628 (31)	9 (0.4)	98 (5)	587 (29)	1266 (63)	796 (40)	0 (0)
Eucalyptus microtheca	266 (13)	113 (6)	8.6 (0.4)	57 (3)	954 (48)	857 (43)	620 (31)	0 (0)
Eucalyptus papuana	31 (2)	148 (7)	2.9 (0.1)	48 (2.4)	306 (15)	888 (44)	252 (13)	0 (0)
Eucalyptus woodwardii	412 (21)	53 (3)	0.93 (0.05)	16.9 (0.8)	678 (34)	239 (12)	107 (5)	882 (44)
Pascopyrum smithii	8.2 (0.4)	36 (2)	13.8 (0.7)	41 (2)	188 (9)	72 (4)	1278 (64)	0 (0)
Elymus elymoides	6.4 (0.3)	10.3 (0.5)	29 (1)	7.9 (0.4)	12 (1)	48 (2)	2667 (133)	132 (7)
Thinopyrum intermedium	18.8 (0.9)	23 (1)	10.7 (0.5)	36 (2)	282 (14)	60 (3)	739 (37)	0 (0)
Bouteloua gracilis	14.3 (0.7)	42 (2)	21 (1)	57 (3)	334 (17)	147 (7)	1696 (85)	51 (3)
Sorghastrum nutans	6.3 (0.3)	22 (1)	17.1 (0.9)	9.8 (0.5)	32 (2)	54 (3)	1508 (75)	75 (4)

Table 7: Unburned foliage concentrations of Cr, Mn, Co, Ni, Cu, Zn, Rb, and Sr. The reagent blank concentration of each trace metal analyzed was subtracted from the unburned foliage samples.

Sample Name	Cr (µg)	Mn (mg)	Co (µg)	Ni (µg)	Cu (µg)	Zn (mg)	Rb (µg)	Sr (µg)
Pinus ponderosa 1	9.6 (0.5)	12.5 (0.6)	17.7 (0.9)	53 (3)	712 (36)	2.2 (0.1)	192 (10)	64 (3)
Pinus ponderosa 2	7.2 (0.4)	12.4 (0.6)	12.5 (0.6)	189 (9)	1040 (52)	3.6 (0.2)	411 (21)	96 (5)
Pinus ponderosa 3	12.1 (0.6)	14 (0.7)	21 (1)	33 (2)	523 (26)	2 (0.1)	152 (8)	149 (7)
Pinus ponderosa 4	8.4 (0.4)	14.7 (0.7)	23 (1)	55 (3)	754 (38)	2.5 (0.1)	205 (10)	110 (6)
Arenga pinnata	0 (0)	0.69 (0.03)	0 (0)	5.1 (0.3)	558 (28)	0.61 (0.03)	28 (1)	1036 (52)
Bambusa spp.	1.84 (0.09)	0.34 (0.02)	1.39 (0.07)	3 (0.2)	239 (12)	0.4 (0.02)	109 (5)	222 (11)
Cissus sicyoides	0.26 (0.01)	0.53 (0.03)	0 (0)	2.2 (0.1)	197 (10)	0.19 (0.01)	43 (2)	3382 (169)
Costas spp.	0.75 (0.04)	9.7 (0.5)	0 (0)	7.4 (0.4)	85 (4)	0.25 (0.01)	84 (4)	917 (46)
Elaeis guianensis	133 (7)	3.6 (0.2)	978 (49)	33 (2)	305 (15)	1.44 (0.07)	111 (6)	1100 (55)
Inga spp.	3.8 (0.2)	2.3 (0.1)	11.1 (0.6)	3.7 (0.2)	214 (11)	0.46 (0.02)	95 (5)	1178 (59)
Melia azedarach	0 (0)	3.2 (0.2)	32 (2)	10.7 (0.5)	127 (6)	0.55 (0.03)	126 (6)	4008 (200)
Musa spp.	3.2 (0.2)	2.1 (0.1)	0 (0)	6.5 (0.3)	145 (7)	0.45 (0.02)	48 (2)	1623 (81)
Pachira aquatica	0 (0)	1.2 (0.06)	0 (0)	10.9 (0.5)	123 (6)	0.32 (0.02)	31 (2)	1903 (95)
Spathodea campanulata	0 (0)	0.35 (0.02)	0 (0)	6 (0.3)	197 (10)	0.23 (0.01)	89 (4)	761 (38)
Eucalyptus camaldulensis	9.9 (0.5)	17.5 (0.9)	0 (0)	129 (6)	260 (13)	5.7 (0.3)	77 (4)	14740 (740)
Eucalyptus erythrocorys	0 (0)	3.3 (0.2)	BDL	71 (4)	1042 (52)	1.62 (0.08)	87 (4)	11782 (589)
Eucalyptus microtheca	73 (4)	3.6 (0.2)	183 (9)	107 (5)	328 (16)	1.43 (0.07)	177 (9)	5757 (288)
Eucalyptus papuana	0 (0)	11.5 (0.6)	473 (24)	206 (10)	441 (22)	3.4 (0.2)	81 (4)	5920 (296)
Eucalyptus woodwardii	163 (8)	1.51 (0.08)	427 (21)	BDL	55 (3)	0.3 (0.01)	60 (3)	2348 (117)
Pascopyrum smithii	5.2 (0.3)	1.46 (0.07)	BDL	22 (1)	174 (9)	0.45 (0.02)	122 (6)	486 (24)
Elymus elymoides	17.9 (0.9)	0.62 (0.03)	29 (1)	9 (0.4)	81 (4)	0.35 (0.02)	22 (1)	466 (23)
Thinopyrum intermedium	3.6 (0.2)	1.34 (0.07)	BDL	5.7 (0.3)	111 (6)	0.53 (0.03)	203 (10)	383 (19)
Bouteloua gracilis	18.7 (0.9)	1.85 (0.09)	BDL	2.7 (0.1)	259 (13)	0.69 (0.03)	230 (11)	942 (47)
Sorghastrum nutans	327 (16)	0.7 (0.04)	816 (41)	45 (2)	116 (6)	0.26 (0.01)	33 (2)	431 (22)

Table 8: Unburned foliage concentrations of Zr, Mo, Cd, Cs, Ba, La, Ce, and Pr. The reagent blank concentration of each trace metal analyzed was subtracted from the unburned foliage samples.

Sample Name	Zr (µg)	Mo (µg)	Cd (µg)	Cs (µg)	Ba (µg)	La (µg)	Ce (µg)	Pr (ng)
Pinus ponderosa 1	0.74 (0.04)	14.6 (0.7)	10.3 (0.5)	1.04 (0.05)	98 (5)	4.7 (0.2)	8.9 (0.4)	1084 (54)
Pinus ponderosa 2	2.7 (0.1)	15 (0.7)	15.5 (0.8)	1.81 (0.09)	105 (5)	5.2 (0.3)	9.7 (0.5)	1148 (57)
Pinus ponderosa 3	2.3 (0.1)	23 (1)	10.7 (0.5)	1.54 (0.08)	124 (6)	8 (0.4)	13.7 (0.7)	1774 (89)
Pinus ponderosa 4	1.21 (0.06)	17.2 (0.9)	11 (0.5)	1.76 (0.09)	94 (5)	6 (0.3)	10.7 (0.5)	1330 (66)
Arenga pinnata	2.8 (0.1)	8.4 (0.4)	2.4 (0.1)	0.25 (0.01)	652 (33)	0.29 (0.01)	0.44 (0.02)	69 (3)
Bambusa spp.	0.08 (0.004)	42 (2)	0.101 (0.005)	0.36 (0.02)	314 (16)	0.044 (0.002)	0.08 (0.004)	8 (0)
Cissus sicyoides	3.6 (0.2)	388 (19)	0.146 (0.007)	0.47 (0.02)	1047 (52)	0.67 (0.03)	0.86 (0.04)	79 (4)
Costas spp.	2.9 (0.1)	180 (9)	0.38 (0.02)	1.04 (0.05)	1124 (56)	0.86 (0.04)	1.77 (0.09)	140 (7)
Elaeis guianensis	2.03 (0.1)	90 (5)	0.48 (0.02)	3.5 (0.2)	380 (19)	0.22 (0.01)	0.37 (0.02)	44 (2)
Inga spp.	1.3 (0.07)	107 (5)	0.59 (0.03)	4.2 (0.2)	264 (13)	0.087 (0.004)	0.088 (0.004)	14 (1)
Melia azedarach	28 (1)	114 (6)	0.15 (0.008)	1.9 (0.1)	1363 (68)	1.46 (0.07)	2.3 (0.1)	227 (11)
Musa spp.	0.77 (0.04)	108 (5)	0.067 (0.003)	0.86 (0.04)	995 (50)	0.22 (0.01)	0.45 (0.02)	49 (2)
Pachira aquatica	0.57 (0.03)	1.71 (0.09)	0.28 (0.01)	0.42 (0.02)	562 (28)	0.69 (0.03)	1.3 (0.06)	111 (6)
Spathodea campanulata	3.7 (0.2)	17.6 (0.9)	0.23 (0.01)	0.92 (0.05)	534 (27)	0.22 (0.01)	0.27 (0.01)	29 (1)
Eucalyptus camaldulensis	37 (2)	8.9 (0.4)	4.7 (0.2)	3.8 (0.2)	3859 (193)	17.7 (0.9)	35 (2)	3680 (184)
Eucalyptus erythrocorys	38 (2)	118 (6)	0.61 (0.03)	2.2 (0.1)	2827 (141)	8.3 (0.4)	16.2 (0.8)	1730 (87)
Eucalyptus microtheca	33 (2)	22 (1)	0.5 (0.02)	1.6 (0.08)	818 (41)	7 (0.4)	14.5 (0.7)	1520 (76)
Eucalyptus papuana	2.1 (0.1)	5 (0.3)	5.6 (0.3)	0.76 (0.04)	1466 (73)	3.2 (0.2)	6.2 (0.3)	677 (34)
Eucalyptus woodwardii	22 (1)	1.45 (0.07)	1.38 (0.07)	BDL	138 (7)	0.88 (0.04)	1.8 (0.09)	192 (10)
Pascopyrum smithii	18.2 (0.9)	7.3 (0.4)	0.72 (0.04)	0.85 (0.04)	557 (28)	9.2 (0.5)	17.2 (0.9)	1864 (93)
Elymus elymoides	545 (27)	7.4 (0.4)	0.68 (0.03)	1.46 (0.07)	1336 (67)	26 (1)	50 (3)	5406 (270)
Thinopyrum intermedium	21 (1)	12.4 (0.6)	0.66 (0.03)	2 (0.1)	537 (27)	5.4 (0.3)	10.2 (0.5)	1096 (55)
Bouteloua gracilis	110 (6)	63 (3)	0.59 (0.03)	1.83 (0.09)	1295 (65)	11.7 (0.6)	23 (1)	2470 (123)
Sorghastrum nutans	30 (1)	30 (1)	0.44 (0.02)	1.21 (0.06)	629 (31)	13.4 (0.7)	27 (1)	2928 (146)

Table 9: Unburned foliage concentrations of Nd, Sm, Eu, Gd, Tb, Dy, Ho, Er, and Tm. The reagent blank concentration of each trace metal analyzed was subtracted from the unburned foliage samples.

Sample Name	Nd (μg)	Sm (ng)	Eu (ng)	Gd (ng)	Tb (ng)	Dy (ng)	Ho (ng)	Er (ng)	Tm (ng)
Pinus ponderosa 1	4.5 (0.2)	911 (46)	203 (10)	849 (42)	139 (7)	864 (43)	178 (9)	505 (25)	65 (3)
Pinus ponderosa 2	4.7 (0.2)	901 (45)	195 (10)	836 (42)	133 (7)	816 (41)	173 (9)	496 (25)	64 (3)
Pinus ponderosa 3	7.2 (0.4)	1382 (69)	290 (15)	1253 (63)	197 (10)	1199 (60)	248 (12)	705 (35)	94 (5)
Pinus ponderosa 4	5.4 (0.3)	1038 (52)	221 (11)	943 (47)	148 (7)	905 (45)	190 (9)	536 (27)	71 (4)
Arenga pinnata	0.33 (0.02)	72 (4)	44 (2)	87 (4)	15.2 (0.8)	94 (5)	19 (1)	57 (3)	8.3 (0.4)
Bambusa spp.	0.033 (0.002)	9 (0)	13.6 (0.7)	7.1 (0.4)	2 (0.1)	9.6 (0.5)	2.6 (0.1)	7.1 (0.4)	1.4 (0.1)
Cissus sicyoides	0.3 (0.01)	53 (3)	45 (2)	58 (3)	8 (0.4)	36 (2)	8.8 (0.4)	19 (1)	2.5 (0.1)
Costas spp.	0.59 (0.03)	129 (6)	62 (3)	156 (8)	25 (1)	153 (8)	30 (2)	86 (4)	11.4 (0.6)
Elaeis guianensis	0.178 (0.009)	45 (2)	23 (1)	45 (2)	7.6 (0.4)	46 (2)	11.1 (0.6)	35 (2)	4.8 (0.2)
Inga spp.	0.062 (0.003)	12 (1)	12.4 (0.6)	16.2 (0.8)	2.3 (0.1)	20 (1)	4.6 (0.2)	13.3 (0.7)	1.9 (0.1)
Melia azedarach	0.92 (0.05)	167 (8)	78 (4)	178 (9)	25 (1)	140 (7)	29 (1)	75 (4)	9.4 (0.5)
Musa spp.	0.185 (0.009)	60 (3)	41 (2)	39 (2)	6.8 (0.3)	34 (2)	8.5 (0.4)	26 (1)	3.7 (0.2)
Pachira aquatica	0.47 (0.02)	84 (4)	83 (4)	95 (5)	19 (1)	73 (4)	15.2 (0.8)	40 (2)	5 (0.3)
Spathodea campanulata	0.122 (0.006)	25 (1)	22 (1)	27 (1)	3.7 (0.2)	22 (1)	4.8 (0.2)	11 (0.6)	1.5 (0.1)
Eucalyptus camaldulensis	14.4 (0.7)	2647 (132)	626 (31)	2380 (119)	337 (17)	1928 (96)	380 (19)	1073 (54)	154 (8)
Eucalyptus erythrocorys	6.6 (0.3)	1171 (59)	641 (32)	1048 (52)	149 (7)	916 (46)	187 (9)	587 (29)	90 (5)
Eucalyptus microtheca	5.9 (0.3)	1020 (51)	321 (16)	932 (47)	144 (7)	884 (44)	166 (8)	494 (25)	79 (4)
Eucalyptus papuana	2.6 (0.1)	442 (22)	288 (14)	412 (21)	59 (3)	349 (17)	66 (3)	192 (10)	29 (1)
Eucalyptus woodwardii	0.82 (0.04)	119 (6)	BDL	108 (5)	BDL	86 (4)	23 (1)	66 (3)	BDL
Pascopyrum smithii	7.4 (0.4)	1270 (64)	389 (19)	1113 (56)	157 (8)	895 (45)	168 (8)	466 (23)	67 (3)
Elymus elymoides	21.31 (1.07)	3707 (185)	1015 (51)	3249 (162)	465 (23)	2616 (131)	494 (25)	1410 (71)	196 (10)
Thinopyrum intermedium	4.3 (0.2)	769 (38)	251 (13)	667 (33)	96 (5)	596 (30)	115 (6)	338 (17)	51 (3)
Bouteloua gracilis	9.7 (0.5)	1745 (87)	565 (28)	1475 (74)	212 (11)	1248 (62)	249 (12)	707 (35)	105 (5)
Sorghastrum nutans	11.9 (0.6)	2179 (109)	550 (27)	1842 (92)	269 (13)	1569 (78)	303 (15)	861 (43)	120 (6)

Table 10: Unburned foliage concentrations of Yb, Lu, Hf, W, Re, Pb, Th, and U. The reagent blank concentration of each trace metal analyzed was subtracted from the unburned foliage samples.

Sample Name	Yb (ng)	Lu (ng)	Hf (ng)	W (ng)	Re (ng)	Pb (µg)	Th (ng)	U (µg)
Pinus ponderosa 1	394 (20)	59 (3)	11 (0.6)	644 (32)	60 (3)	10 (0.5)	883 (44)	0.34 (0.02)
Pinus ponderosa 2	383 (19)	58 (3)	26 (1)	702 (35)	32 (2)	11.8 (0.6)	1175 (59)	0.34 (0.02)
Pinus ponderosa 3	569 (28)	86 (4)	28 (1)	1096 (55)	69 (3)	13 (0.7)	1382 (69)	0.49 (0.02)
Pinus ponderosa 4	432 (22)	66 (3)	43 (2)	1022 (51)	66 (3)	13.7 (0.7)	999 (50)	0.38 (0.02)
Arenga pinnata	44 (2)	7.2 (0.4)	109 (5)	1029 (51)	59 (3)	5.6 (0.3)	4.1 (0.2)	5.6 (0.3)
Bambusa spp.	12.9 (0.6)	2.7 (0.1)	9.1 (0.5)	1789 (89)	80 (4)	1.57 (0.08)	4.3 (0.2)	0.024 (0.001)
Cissus sicyoides	11.9 (0.6)	2.2 (0.1)	93 (5)	19376 (969)	132 (7)	4.1 (0.2)	37 (2)	BDL
Costas spp.	61 (3)	8.4 (0.4)	63 (3)	3157 (158)	0 (0)	1.85 (0.09)	18.1 (0.9)	0.31 (0.02)
Elaeis guianensis	31 (2)	6.1 (0.3)	53 (3)	3737 (187)	40 (2)	4.3 (0.2)	5.5 (0.3)	0.85 (0.04)
Inga spp.	12 (0.6)	1.9 (0.1)	27 (1)	559 (28)	65 (3)	1.9 (0.1)	8.2 (0.4)	0.51 (0.03)
Melia azedarach	55 (3)	9.1 (0.5)	552 (28)	3030 (151)	534 (27)	8.2 (0.4)	30 (2)	0.89 (0.04)
Musa spp.	29 (1)	5.7 (0.3)	84 (4)	1150 (58)	202 (10)	3.2 (0.2)	31 (2)	1.81 (0.09)
Pachira aquatica	27 (1)	3.9 (0.2)	44 (2)	244 (12)	60 (3)	7.4 (0.4)	14.3 (0.7)	0.94 (0.05)
Spathodea campanulata	8.6 (0.4)	1.4 (0.1)	78 (4)	569 (28)	75 (4)	1.28 (0.06)	10.2 (0.5)	0.79 (0.04)
Eucalyptus camaldulensis	1018 (51)	154 (8)	938 (47)	1456 (73)	4837 (242)	20.82 (1.04)	3434 (172)	7.2 (0.4)
Eucalyptus erythrocorys	628 (31)	82 (4)	1135 (57)	286 (14)	5218 (261)	19 (1)	1735 (87)	2.6 (0.1)
Eucalyptus microtheca	513 (26)	80 (4)	1016 (51)	525 (26)	2353 (118)	13.7 (0.7)	1983 (99)	0.84 (0.04)
Eucalyptus papuana	190 (10)	28 (1)	114 (6)	0 (0)	868 (43)	6.7 (0.3)	640 (32)	1.68 (0.08)
Eucalyptus woodwardii	56 (3)	BDL	562 (28)	0 (0)	224 (11)	6 (0.3)	582 (29)	0.19 (0.01)
Pascopyrum smithii	430 (21)	62 (3)	463 (23)	149 (7)	2.1 (0.1)	8.1 (0.4)	1026 (51)	0.41 (0.02)
Elymus elymoides	1276 (64)	179 (9)	11601 (580)	506 (25)	0 (0)	19 (1)	3661 (183)	1.13 (0.06)
Thinopyrum intermedium	340 (17)	51 (3)	188 (9)	204 (10)	136 (7)	6.9 (0.3)	1215 (61)	0.4 (0.02)
Bouteloua gracilis	661 (33)	102 (5)	2482 (124)	1102 (55)	31 (2)	9.5 (0.5)	2370 (118)	0.67 (0.03)
Sorghastrum nutans	797 (40)	112 (6)	778 (39)	843 (42)	0 (0)	8.3 (0.4)	1968 (98)	0.69 (0.03)

APPENDIX F

DATA: TRACE METALS IN COARSE AEROSOLS

Table 11: Coarse fraction field blank aerosol concentrations of Na, Mg, Al, P, K, and Ca. The average filter blank concentration of each trace metal was subtracted from the field blanks.

Field Blank	Na (μg)	Mg (μg)	Al (μg)	P (μg)	K (μg)	Ca (μg)
1	0 (5.1)	0.23 (0.31)	1.1 (0.6)	0 (0.04)	0 (0.2)	0 (0)
2	0 (5.1)	0.85 (0.31)	2.8 (0.6)	0.34 (0.06)	1.3 (0.2)	0.7 (0.2)
3	0.8 (0.5)	0.37 (0.02)	0 (0)	0.21 (0.05)	0.9 (0.04)	BDL
4	1.2 (0.5)	0.023 (0.001)	1.81 (0.09)	0.34 (0.06)	1 (0.1)	BDL
5	0.1 (0.5)	0.18 (0.01)	0 (0)	0.13 (0.05)	0.39 (0.02)	BDL
6	0.6 (0.5)	0.32 (0.02)	0 (0)	0.29 (0.05)	0.84 (0.04)	BDL
7	2.1 (0.5)	0.057 (0.003)	0 (0)	0.22 (0.05)	2.5 (0.1)	BDL
8	1.1 (1.5)	0.99 (0.59)	6.6 (0.8)	0 (0.2)	2.1 (0.3)	1.6 (0.3)
9	1.5 (1.5)	0.24 (0.58)	16.2 (1.1)	0.38 (0.21)	0.9 (0.3)	0.2 (0.3)
10	2.6 (1.5)	0.17 (0.58)	12 (0.9)	0 (0.21)	0.3 (0.3)	2.2 (0.3)
11	0.9 (1.4)	0.73 (0.59)	4.6 (0.8)	0.36 (0.21)	1.5 (0.3)	1.6 (0.3)

Table 12: Coarse fraction field blank aerosol concentrations of Ti, V, Cr, Mn, Co, and Ni. The average filter blank concentration of each trace metal was subtracted from the field blanks.

Field Blank	Ti (μg)	V (ng)	Cr (ng)	Mn (μg)	Co (ng)	Ni (ng)
1	0.1 (0.02)	0 (11)	18675 (1051)	0.58 (0.04)	32958 (1649)	1011 (51)
2	0.13 (0.02)	0 (11)	0 (463)	0.11 (0.02)	0 (26)	7 (5)
3	0 (0)	0 (3)	0 (0)	0.044 (0.002)	0.4 (0.2)	8 (11)
4	0.37 (0.02)	8 (3)	61 (3)	0.024 (0.001)	0.3 (0.2)	5 (11)
5	0 (0)	2 (3)	0 (0)	0.009 (0)	0 (0.2)	14 (11)
6	0 (0)	0 (3)	0 (0)	0.018 (0.001)	0.2 (0.2)	5 (11)
7	0 (0)	0 (3)	0 (0)	0.011 (0.001)	0 (0.2)	0 (11)
8	0.46 (0.12)	4 (1)	20 (51)	0.073 (0.009)	1 (0.5)	1 (51)
9	0.05 (0.12)	4 (1)	0 (51)	0.018 (0.008)	0.1 (0.5)	0 (51)
10	0.12 (0.12)	5 (1)	75 (52)	0.014 (0.008)	0.4 (0.5)	15 (51)
11	0.15 (0.12)	0 (1)	4 (51)	0.06 (0.009)	0.6 (0.5)	0 (51)

Table 13: Coarse fraction field blank aerosol concentrations of Cu, Zn, Rb, Sr, Zr, and Mo. The average filter blank concentration of each trace metal was subtracted from the field blanks.

Field Blank	Cu (ng)	Zn (µg)	Rb (ng)	Sr (ng)	Zr (ng)	Mo (ng)
1	BDL	0 (1)	1.2 (0.1)	BDL	6 (1)	0.5 (0.4)
2	BDL	0 (1)	3.6 (0.2)	14 (1)	2 (1)	0 (0.4)
3	BDL	0.47 (0.02)	3.2 (0.2)	5 (0)	0 (0)	0 (0.6)
4	BDL	0.153 (0.008)	1.47 (0.07)	12 (1)	1.34 (0.07)	0 (0.6)
5	BDL	0.149 (0.007)	0 (0)	6.1 (0.3)	0.51 (0.03)	0.7 (0.6)
6	BDL	0.159 (0.008)	0 (0)	BDL	0 (0)	1.3 (0.6)
7	BDL	0.29 (0.01)	0 (0)	BDL	0 (0)	0 (0.6)
8	271 (14)	1.2 (0.1)	5 (4)	9 (5)	2 (2)	1 (2)
9	64 (3)	0 (0)	6 (4)	0 (5)	3 (2)	0.5 (2)
10	79 (4)	0 (0)	0 (4)	12 (5)	3 (2)	0.6 (2)
11	106 (5)	0 (0)	3 (4)	5 (5)	6 (3)	3 (2)

Table 14: Coarse fraction field blank aerosol concentrations of Cd, Cs, Ba, La, Ce, and Pr. The average filter blank concentration of each trace metal was subtracted from the field blanks.

Field Blank	Cd (ng)	Cs (ng)	Ba (µg)	La (ng)	Ce (ng)	Pr (ng)
1	BDL	0.157 (0.008)	0.06 (0.01)	1 (0.3)	2.3 (0.6)	0.22 (0.01)
2	0.157 (0.008)	0.33 (0.02)	0.03 (0.01)	1.8 (0.3)	4.3 (0.6)	0.41 (0.02)
3	BDL	0.46 (0.02)	0.05 (0.01)	0 (0)	0 (0)	0 (0)
4	BDL	0.207 (0.01)	0.02 (0.01)	0.33 (0.02)	0 (0)	0.07 (0)
5	BDL	0.08 (0.004)	0 (0.01)	0 (0)	0 (0)	0 (0)
6	BDL	0.061 (0.003)	0.01 (0.01)	0 (0)	0 (0)	0 (0)
7	0 (0)	0.02 (0.001)	0.04 (0.01)	0 (0)	0 (0)	0 (0)
8	0.57 (0.04)	0.3 (0.2)	0.06 (0.01)	1.6 (0.7)	4 (1)	0.36 (0.1)
9	0.17 (0.02)	0.3 (0.2)	0.04 (0.01)	1.4 (0.7)	3 (1)	0.24 (0.1)
10	BDL	0.1 (0.2)	0.01 (0.01)	0.6 (0.7)	1 (1)	0.18 (0.09)
11	0.018 (0.008)	0.3 (0.2)	0.04 (0.01)	1.6 (0.7)	3 (1)	0.39 (0.1)

Table 15: Coarse fraction field blank aerosol concentrations of Nd, Sm, Eu, Gd, Tb, and Dy. The average filter blank concentration of each trace metal was subtracted from the field blanks.

Field Blank	Nd (ng)	Sm (ng)	Eu (ng)	Gd (ng)	Tb (ng)	Dy (ng)
1	1 (0.2)	0.19 (0.01)	0.045 (0.002)	0.15 (0.01)	BDL	0.11 (0.01)
2	1.6 (0.2)	0.32 (0.02)	0.083 (0.004)	0.3 (0.01)	0.036 (0.002)	0.24 (0.01)
3	0 (0)	0 (0)	0.01 (0.001)	0 (0)	0 (0)	0 (0)
4	0.4 (0)	0.1 (0.01)	0.026 (0.001)	0.06 (0)	0.002 (0)	0.01 (0)
5	0 (0)	0 (0)	0 (0)	0 (0)	0 (0)	0 (0)
6	0 (0)	0 (0)	0 (0)	0 (0)	BDL	0 (0)
7	0 (0)	0 (0)	BDL	0 (0)	BDL	BDL
8	1.5 (0.6)	0.25 (0.03)	0.05 (0.03)	0.21 (0.07)	0.067 (0.003)	0.26 (0.05)
9	0.9 (0.6)	0.1 (0.03)	0 (0.03)	0.1 (0.07)	0.071 (0.004)	0.09 (0.05)
10	0.6 (0.6)	0.22 (0.03)	0.01 (0.03)	0.07 (0.07)	0.05 (0.002)	0.15 (0.05)
11	1.5 (0.6)	0.28 (0.03)	0.05 (0.03)	0.22 (0.07)	BDL	0.19 (0.05)

Table 16: Coarse fraction field blank aerosol concentrations of Ho, Er, Tm, Yb, and Lu. The average filter blank concentration of each trace metal was subtracted from the field blanks.

Field Blank	Ho (ng)	Er (ng)	Tm (ng)	Yb (ng)	Lu (ng)
1	0.032 (0.002)	0.056 (0.003)	BDL	0.045 (0.003)	0.007 (0)
2	0.052 (0.003)	0.157 (0.008)	0.02 (0.001)	0.108 (0.006)	0.02 (0.001)
3	0 (0)	0 (0)	0 (0)	0 (0)	0 (0)
4	0 (0)	0 (0)	0 (0)	0.042 (0.002)	0 (0)
5	0 (0)	0 (0)	0 (0)	0 (0)	0 (0)
6	BDL	0 (0)	0 (0)	0 (0)	BDL
7	BDL	BDL	BDL	BDL	BDL
8	0.089 (0.004)	0.202 (0.01)	0.029 (0.001)	0.15 (0.01)	0.027 (0.001)
9	0.041 (0.002)	0.168 (0.008)	BDL	0.002 (0.005)	BDL
10	0.047 (0.002)	0.171 (0.009)	BDL	BDL	BDL
11	0.066 (0.003)	0.181 (0.009)	0.026 (0.001)	0.12 (0.01)	0.029 (0.001)

Table 17: Coarse fraction field blank aerosol concentrations of Hf, W, Re, Pb, Th, and U. The average filter blank concentration of each trace metal was subtracted from the field blanks.

Field Blank	Hf (ng)	W (ng)	Re (ng)	Pb (ng)	Th (ng)	U (ng)
1	0.09 (0.01)	4 (2)	0 (0)	5 (2)	0.05 (0.02)	BDL
2	0.09 (0.01)	0 (2)	0 (0)	3 (2)	0.04 (0.02)	BDL
3	0 (0)	BDL	BDL	0 (0)	0 (0)	BDL
4	0 (0)	BDL	0 (0)	1.6 (0.1)	0 (0)	0.46 (0.02)
5	0 (0)	BDL	BDL	0 (0)	0 (0)	BDL
6	0 (0)	BDL	BDL	26 (1)	0 (0)	BDL
7	0 (0)	BDL	BDL	0 (0)	0 (0)	BDL
8	0.05 (0.02)	BDL	0 (0)	48 (3)	0.16 (0.01)	0 (0.2)
9	0.09 (0.02)	BDL	0 (0)	3 (1)	0 (0)	0 (0.2)
10	0.07 (0.02)	0 (0)	0 (0)	1 (1)	0 (0)	0 (0.2)
11	0.19 (0.02)	BDL	0 (0)	2 (1)	0.13 (0.01)	0.1 (0.2)

Table 18: Coarse fraction burn aerosol concentrations of Na, Mg, Al, P, K, Ca, and Ti. The average filter blank concentration of each trace metal analyzed was subtracted from the aerosol samples.

Sample Name	Na (µg)	Mg (µg)	Al (µg)	P (µg)	K (µg)	Ca (µg)	Ti (µg)
Pinus ponderosa 1	0 (5)	1.1 (0.3)	39.9 (2)	2.5 (0.2)	29 (2)	0 (0)	0.05 (0.02)
Pinus ponderosa 2	2.3 (5)	75 (4)	23.8 (1)	140 (7)	711 (36)	121 (6)	1.51 (0.08)
Pinus ponderosa 3	0 (5)	78 (4)	4.5 (0.7)	96 (5)	401 (20)	109 (6)	0.77 (0.05)
Pinus ponderosa 4	0 (5)	4.3 (0.4)	0 (0)	6.3 (0.4)	49 (3)	3.5 (0.3)	0.15 (0.02)
Arenga pinnata	0.8 (0.5)	1.09 (0.05)	0 (0)	1.5 (0.1)	7.2 (0.4)	3.5 (0.2)	0 (0)
Bambusa spp.	0.9 (0.5)	0.78 (0.04)	0.34 (0.01)	0.84 (0.08)	15.1 (0.8)	BDL	0 (0)
Cissus sicyoides	1.6 (0.5)	1.89 (0.09)	0 (0)	1.3 (0.1)	10.1 (0.5)	5.7 (0.3)	0 (0)
Costas spp.	0.3 (0.5)	2.1 (0.1)	0 (0)	1.3 (0.1)	16.2 (0.8)	10.6 (0.5)	0 (0)
Elaeis guianensis	1.7 (0.5)	6.1 (0.3)	0 (0)	3.2 (0.2)	47 (2)	14.4 (0.7)	0 (0)
Inga spp.	0.2 (0.5)	2.5 (0.1)	0 (0)	1.9 (0.1)	8.8 (0.4)	15.1 (0.8)	0 (0)
Melia azedarach	1.5 (0.5)	81 (4)	0 (0)	21 (1)	101 (5)	109 (5)	0 (0)
Musa spp.	0 (0.5)	3.4 (0.2)	0 (0)	2.8 (0.2)	49 (2)	32 (2)	0 (0)
Pachira aquatica	0.3 (0.5)	1.69 (0.08)	0 (0)	1.03 (0.09)	10.7 (0.5)	21 (1)	0 (0)
Spathodea campanulata	0 (0.5)	0.65 (0.03)	3.3 (0.1)	0.36 (0.06)	5.0 (0.2)	0.81 (0.04)	0 (0)
Eucalyptus camaldulensis	10.7 (0.8)	40 (2)	1.2 (0.7)	11.4 (0.6)	113 (6)	150 (8)	0 (0)
Eucalyptus erythrocorys	15 (2)	4.4 (0.6)	13.9 (1)	0.8 (0.2)	22 (1)	2.9 (0.3)	0.1 (0.1)
Eucalyptus microtheca	3 (2)	0.7 (0.6)	12.8 (1)	0 (0.2)	17.8 (0.9)	1.9 (0.3)	0.1 (0.1)
Eucalyptus papuana	3 (2)	4.5 (0.6)	5.3 (0.8)	2.2 (0.2)	49 (3)	14.0 (0.8)	0.1 (0.1)
Eucalyptus woodwardii	21 (2)	4.3 (0.6)	5.4 (0.8)	1.7 (0.2)	20 (1)	18 (1)	0.1 (0.1)
Pascopyrum smithii	2 (2)	2.3 (0.6)	16.5 (1)	0.9 (0.2)	4.3 (0.4)	5.0 (0.4)	0.5 (0.1)
Elymus elymoides	3 (2)	3.7 (0.6)	63.9 (3)	1.6 (0.2)	9.8 (0.6)	9.1 (0.5)	1 (0.1)
Thinopyrum intermedium	4 (2)	8.2 (0.7)	18.2 (1)	9.3 (0.5)	54 (3)	22 (1)	0.8 (0.1)
Bouteloua gracilis	3 (2)	3.7 (0.6)	7.3 (0.8)	0.9 (0.2)	3.9 (0.4)	10 .0(0.6)	1.6 (0.1)
Sorghastrum nutans	0 (1)	3.5 (0.6)	39.9 (2)	1.6 (0.2)	10.9 (0.6)	5.0 (0.4)	0.6 (0.1)

Table 19: Coarse fraction burn aerosol concentrations of V, Cr, Mn, Co, Ni, Cu, and Zn. The average filter blank concentration of each trace metal analyzed was subtracted from the aerosol samples.

Sample Name	V (ng)	Cr (ng)	Mn (μg)	Co (ng)	Ni (ng)	Cu (ng)	Zn (μg)
Pinus ponderosa 1	0 (11)	0 (463)	0.42 (0.03)	0 (26)	110 (8)	BDL	0 (1)
Pinus ponderosa 2	37 (11)	0 (463)	24 (1)	6 (26)	95 (7)	BDL	3.4 (0.7)
Pinus ponderosa 3	18 (11)	0 (463)	16.2 (0.8)	19 (26)	37 (5)	BDL	1.5 (0.6)
Pinus ponderosa 4	8 (11)	0 (463)	1.06 (0.06)	1 (26)	0 (5)	BDL	0 (0.6)
Arenga pinnata	0 (3)	0 (0)	0.041 (0.002)	0 (0.2)	5 (11)	BDL	0.60 (0.03)
Bambusa spp.	0 (3)	0 (0)	0.023 (0.001)	0 (0.2)	4 (11)	BDL	0.78 (0.04)
Cissus sicyoides	0 (3)	0 (0)	0.067 (0.003)	0.9 (0.2)	5 (11)	BDL	0.30 (0.02)
Costas spp.	0 (3)	0 (0)	0.34 (0.02)	0.4 (0.2)	1 (11)	BDL	0.26 (0.01)
Elaeis guianensis	0 (3)	0 (0)	0.15 (0.008)	0.3 (0.2)	5 (11)	BDL	0.26 (0.01)
Inga spp.	0 (3)	0 (0)	0.089 (0.004)	0 (0.2)	5 (11)	BDL	0.172 (0.009)
Melia azedarach	0 (3)	0 (0)	0.82 (0.04)	8.2 (0.4)	19 (11)	BDL	0.29 (0.01)
Musa spp.	1 (3)	0 (0)	0.30 (0.02)	0 (0.2)	0 (11)	BDL	0.146 (0.007)
Pachira aquatica	4 (3)	0 (0)	0.07 (0.004)	0.3 (0.2)	14 (11)	BDL	0.176 (0.009)
Spathodea campanulata	6 (3)	0 (0)	0.033 (0.002)	0 (0.2)	1 (11)	BDL	5.2 (0.3)
Eucalyptus camaldulensis	16 (3)	0 (0)	1.16 (0.06)	0.7 (0.2)	20 (11)	BDL	2.6 (0.1)
Eucalyptus erythrocorys	6 (1)	0 (51)	0.042 (0.009)	0.4 (0.5)	0 (51)	70 (4)	0.3 (0.1)
Eucalyptus microtheca	1.6 (0.9)	0 (51)	0.031 (0.009)	0 (0.5)	0 (51)	BDL	0.1 (0.1)
Eucalyptus papuana	8 (1)	0 (51)	0.28 (0.02)	16 (1)	0 (51)	48 (2)	0.3 (0.1)
Eucalyptus woodwardii	7 (1)	0 (51)	0.25 (0.02)	0.1 (0.5)	0 (51)	21 (1)	0.5 (0.1)
Pascopyrum smithii	10 (1)	0 (51)	0.075 (0.009)	1.1 (0.5)	0 (51)	BDL	0.2 (0.1)
Elymus elymoides	25 (2)	0 (51)	0.17 (0.01)	2.7 (0.5)	0 (51)	28 (1)	0.1 (0.1)
Thinopyrum intermedium	26 (2)	62 (51)	0.34 (0.02)	4.1 (0.6)	21 (51)	46 (2)	0.1 (0.1)
Bouteloua gracilis	31 (2)	0 (51)	0.18 (0.01)	3.9 (0.6)	0 (51)	BDL	0.0 (0.1)
Sorghastrum nutans	10 (1)	0 (51)	0.14 (0.01)	1.5 (0.5)	0 (51)	92 (5)	0 (0)

Table 20: Coarse fraction burn aerosol concentrations of Rb, Sr, Zr, Mo, Cd, Cs, and Ba. The average filter blank concentration of each trace metal analyzed was subtracted from the aerosol samples.

Sample Name	Rb (ng)	Sr (ng)	Zr (ng)	Mo (ng)	Cd (ng)	Cs (ng)	Ba (μg)
Pinus ponderosa 1	13 (1)	BDL	7 (1)	0 (0.4)	3.2 (0.2)	0.108 (0.005)	0.00 (0.01)
Pinus ponderosa 2	235 (12)	135 (7)	19 (2)	7 (0.5)	22 (1)	2.8 (0.1)	0.22 (0.02)
Pinus ponderosa 3	119 (6)	114 (6)	16 (2)	3.4 (0.4)	10.6 (0.5)	1.29 (0.07)	0.11 (0.01)
Pinus ponderosa 4	25 (1)	14.4 (0.7)	8 (1)	0 (0.4)	2.9 (0.1)	0.46 (0.02)	0.03 (0.01)
Arenga pinnata	1.09 (0.05)	16.2 (0.8)	0 (0)	0 (0.6)	1.07 (0.05)	0.170 (0.008)	0.02 (0.01)
Bambusa spp.	4.2 (0.2)	4.6 (0.2)	0 (0)	0 (0.6)	0 (0)	0.115 (0.006)	0.02 (0.01)
Cissus sicyoides	6.6 (0.3)	38 (2)	0 (0)	3 (0.6)	0 (0)	0.50 (0.03)	0.05 (0.01)
Costas spp.	5.7 (0.3)	33 (2)	0 (0)	1.3 (0.6)	0 (0)	0.179 (0.009)	0.07 (0.01)
Elaeis guianensis	8.9 (0.4)	32 (2)	0 (0)	4.2 (0.6)	0.43 (0.02)	0.54 (0.03)	0.02 (0.01)
Inga spp.	2.3 (0.1)	51 (3)	0 (0)	3.6 (0.6)	0.138 (0.007)	0.170 (0.009)	0.01 (0.01)
Melia azedarach	17 (1)	613 (31)	0 (0)	25 (1)	0.0097 (0.0005)	0.26 (0.01)	0.38 (0.02)
Musa spp.	0 (0)	115 (6)	0 (0)	3.3 (0.6)	BDL	0 (0)	0.08 (0.01)
Pachira aquatica	0.98 (0.05)	97 (5)	0 (0)	1.3 (0.6)	0.114 (0.006)	0.050 (0.002)	0.04 (0.01)
Spathodea campanulata	2.2 (0.1)	12.3 (0.6)	0 (0)	0 (0.6)	BDL	0.157 (0.008)	0.02 (0.01)
Eucalyptus camaldulensis	18 (1)	1155 (58)	4.8 (0.2)	0 (0.6)	3.2 (0.2)	0.95 (0.05)	0.36 (0.02)
Eucalyptus erythrocorys	5 (4)	29 (5)	7 (3)	12 (2)	0.12 (0.01)	0.2 (0.2)	0.02 (0.01)
Eucalyptus microtheca	7 (4)	19 (5)	1 (2)	0.9 (2)	0.51 (0.03)	0.2 (0.2)	0.01 (0.01)
Eucalyptus papuana	24 (5)	106 (7)	5 (3)	0 (2)	4.9 (0.3)	0.2 (0.2)	0.05 (0.01)
Eucalyptus woodwardii	6 (4)	141 (9)	7 (3)	2 (2)	1.9 (0.1)	0 (0.2)	0.04 (0.01)
Pascopyrum smithii	5 (4)	43 (5)	12 (3)	0.3 (2)	0.42 (0.03)	0.1 (0.2)	0.20 (0.02)
Elymus elymoides	19 (4)	91 (7)	20 (3)	3.3 (2)	0.20 (0.02)	0.5 (0.2)	0.14 (0.01)
Thinopyrum intermedium	49 (5)	161 (9)	25 (3)	25 (2)	0.024 (0.008)	0.5 (0.2)	0.16 (0.01)
Bouteloua gracilis	7 (4)	135 (8)	27 (3)	0 (2)	0.49 (0.03)	0.3 (0.2)	0.21 (0.02)
Sorghastrum nutans	9 (4)	60 (6)	15 (3)	0 (2)	0.37 (0.03)	0.0 (0.2)	0.10 (0.01)

Table 21: Coarse fraction burn aerosol concentrations of La, Ce, Pr, Nd, Sm, Eu, and Gd. The average filter blank concentration of each trace metal analyzed was subtracted from the aerosol samples.

Sample Name	La (ng)	Ce (ng)	Pr (ng)	Nd (ng)	Sm (ng)	Eu (ng)	Gd (ng)
Pinus ponderosa 1	0.5 (0.3)	0.9 (0.6)	0.11 (0.01)	0.5 (0.2)	0.075 (0.004)	0.030 (0.001)	0.084 (0.004)
Pinus ponderosa 2	17.7 (0.9)	35 (2)	4.1 (0.2)	16.9 (0.9)	3.2 (0.2)	0.69 (0.03)	2.82 (0.14)
Pinus ponderosa 3	7.7 (0.5)	14.7 (0.9)	1.76 (0.09)	7.1 (0.4)	1.41 (0.07)	0.27 (0.01)	1.24 (0.06)
Pinus ponderosa 4	1.6 (0.3)	3.4 (0.6)	0.32 (0.02)	1.3 (0.2)	0.30 (0.01)	0.068 (0.003)	0.26 (0.01)
Arenga pinnata	0 (0)	0 (0)	0 (0)	0 (0)	0 (0)	0 (0)	0 (0)
Bambusa spp.	0 (0)	0 (0)	0 (0)	0 (0)	0 (0)	0 (0)	0 (0)
Cissus sicyoides	0 (0)	0 (0)	0 (0)	0 (0)	0.056 (0.003)	0.026 (0.001)	0.20 (0.01)
Costas spp.	0 (0)	0 (0)	0 (0)	0 (0)	0 (0)	0 (0)	0 (0)
Elaeis guianensis	0 (0)	0 (0)	0 (0)	0 (0)	0 (0)	0 (0)	0 (0)
Inga spp.	0 (0)	0 (0)	0 (0)	0 (0)	BDL	BDL	0 (0)
Melia azedarach	0 (0)	0 (0)	0 (0)	0 (0)	0 (0)	0.110 (0.005)	0 (0)
Musa spp.	0 (0)	0 (0)	0 (0)	0 (0)	BDL	0 (0)	0 (0)
Pachira aquatica	0 (0)	0 (0)	0 (0)	0 (0)	0 (0)	0.017 (0.001)	0 (0)
Spathodea campanulata	0 (0)	0 (0)	0 (0)	0 (0)	0 (0)	0 (0)	0 (0)
Eucalyptus camaldulensis	2 (0.1)	3.5 (0.2)	0.48 (0.02)	1.9 (0.1)	0.30 (0.01)	0.107 (0.005)	0.25 (0.01)
Eucalyptus erythrocorys	0.7 (0.7)	2 (1)	0.15 (0.09)	0.8 (0.6)	0.2- (0.03)	0.02 (0.03)	0.03 (0.07)
Eucalyptus microtheca	0.7 (0.7)	1 (1)	0.15 (0.09)	0.2 (0.6)	0.10 (0.03)	0.03 (0.03)	0.03 (0.07)
Eucalyptus papuana	0.4 (0.7)	1 (1)	0.11 (0.09)	0.5 (0.6)	0.12 (0.03)	0.00 (0.03)	0.09 (0.07)
Eucalyptus woodwardii	0.8 (0.7)	2 (1)	0.19 (0.09)	0.8 (0.6)	0.21 (0.03)	0.02 (0.03)	0.12 (0.07)
Pascopyrum smithii	2.5 (0.7)	5 (1)	0.6 (0.1)	2.1 (0.6)	0.25 (0.03)	0.10 (0.03)	0.28 (0.07)
Elymus elymoides	5.8 (0.7)	12 (1)	1.2 (0.1)	4.5 (0.6)	0.95 (0.06)	0.26 (0.03)	0.70 (0.08)
Thinopyrum intermedium	5.1 (0.7)	9 (1)	1.1 (0.1)	4.4 (0.6)	0.87 (0.05)	0.19 (0.03)	0.59 (0.08)
Bouteloua gracilis	8.3 (0.8)	16 (1)	1.7 (0.1)	6.9 (0.7)	1.28 (0.07)	0.34 (0.03)	0.99 (0.09)
Sorghastrum nutans	3.7 (0.7)	8 (1)	0.9 (0.1)	2.9 (0.6)	0.54 (0.04)	0.16 (0.03)	0.42 (0.07)

Table 22: Coarse fraction burn aerosol concentrations of Tb, Dy, Ho, Er, Tm, Yb, and Lu. The average filter blank concentration of each trace metal analyzed was subtracted from the aerosol samples.

Sample Name	Tb (ng)	Dy (ng)	Ho (ng)	Er (ng)	Tm (ng)	Yb (ng)	Lu (ng)
Pinus ponderosa 1	BDL	0.06 (0.004)	BDL	0.046 (0.002)	BDL	1.09 (0.06)	0.0081 (0.0004)
Pinus ponderosa 2	0.40 (0.02)	2.70 (0.14)	0.52 (0.03)	1.51 (0.08)	0.19 (0.01)	0.51 (0.03)	0.145 (0.007)
Pinus ponderosa 3	0.20 (0.01)	1.20 (0.06)	0.23 (0.01)	0.75 (0.04)	0.089 (0.004)	0.127 (0.007)	0.073 (0.004)
Pinus ponderosa 4	BDL	0.23 (0.01)	0.042 (0.002)	0.151 (0.008)	0.013 (0.001)	0.019 (0.001)	0.017 (0.001)
Arenga pinnata	0 (0)	0 (0)	0 (0)	0 (0)	0 (0)	0 (0)	0 (0)
Bambusa spp.	0 (0)	0 (0)	0 (0)	0 (0)	BDL	0.027 (0.001)	0 (0)
Cissus sicyoides	0.039 (0.002)	0.053 (0.003)	0 (0)	0 (0)	0.0039 (0.0002)	0 (0)	0 (0)
Costas spp.	0 (0)	0 (0)	0 (0)	0 (0)	0 (0)	BDL	0 (0)
Elaeis guianensis	BDL	0 (0)	0 (0)	BDL	0 (0)	BDL	BDL
Inga spp.	BDL	0 (0)	BDL	BDL	BDL	0 (0)	0 (0)
Melia azedarach	0 (0)	0 (0)	0 (0)	0 (0)	0 (0)	BDL	BDL
Musa spp.	BDL	0 (0)	BDL	BDL	BDL	BDL	BDL
Pachira aquatica	0 (0)	0 (0)	BDL	BDL	BDL	0 (0)	BDL
Spathodea campanulata	BDL	0 (0)	0 (0)	BDL	BDL	0.099 (0.005)	BDL
Eucalyptus camaldulensis	0.040 (0.002)	0.35 (0.02)	0.06 (0.003)	0.17 (0.009)	0.018 (0.001)	0.009 (0.005)	0.0023 (0.0001)
Eucalyptus erythrocorys	0.047 (0.002)	0.09 (0.05)	0.025 (0.001)	0.152 (0.008)	BDL	0.056 (0.008)	0.02 (0.001)
Eucalyptus microtheca	0.048 (0.002)	0.13 (0.05)	0.049 (0.002)	0.14 (0.007)	BDL	0 (0)	BDL
Eucalyptus papuana	BDL	0.03 (0.05)	0.035 (0.002)	0.119 (0.006)	BDL	0 (0)	0.018 (0.001)
Eucalyptus woodwardii	BDL	0.11 (0.05)	0.057 (0.003)	0.149 (0.007)	BDL	0.13 (0.01)	BDL
Pascopyrum smithii	0.052 (0.003)	0.20 (0.05)	0.080 (0.004)	0.23 (0.01)	0.027 (0.001)	0.28 (0.02)	0.029 (0.001)
Elymus elymoides	0.132 (0.007)	0.64 (0.06)	0.15 (0.01)	0.43(0.02)	0.060 (0.003)	0.28 (0.02)	0.056 (0.003)
Thinopyrum intermedium	0.119 (0.006)	0.65 (0.06)	0.12 (0.01)	0.35 (0.02)	0.039 (0.002)	0.43 (0.03)	0.052 (0.003)
Bouteloua gracilis	0.177 (0.009)	0.86 (0.07)	0.20 (0.01)	0.54 (0.03)	0.082 (0.004)	0.15 (0.01)	0.06 (0.003)
Sorghastrum nutans	0.079 (0.004)	0.45 (0.06)	0.093 (0.005)	0.29 (0.01)	0.039 (0.002)	1.09 (0.06)	0.035 (0.002)

Table 23: Coarse fraction burn aerosol concentrations of Hf, W, Re, Pb, Th, and U. The average filter blank concentration of each trace metal analyzed was subtracted from the aerosol samples.

Sample Name	Hf (ng)	W (ng)	Re (ng)	Pb (ng)	Th (ng)	U (ng)
Pinus ponderosa 1	0.19 (0.02)	0 (2)	0 (0)	1 (2)	0.02 (0.02)	BDL
Pinus ponderosa 2	0.61 (0.04)	0 (2)	0 (0)	14 (2)	1.66 (0.09)	0.83 (0.04)
Pinus ponderosa 3	0.43 (0.03)	0 (2)	0 (0)	10 (2)	1.15 (0.06)	0.46 (0.02)
Pinus ponderosa 4	0.19 (0.02)	0 (2)	0 (0)	2 (2)	0.47 (0.03)	BDL
Arenga pinnata	0 (0)	BDL	BDL	0.31 (0.02)	0 (0)	BDL
Bambusa spp.	0 (0)	BDL	BDL	0 (0)	0 (0)	BDL
Cissus sicyoides	0 (0)	BDL	BDL	5.9 (0.3)	0 (0)	BDL
Costas spp.	0 (0)	BDL	BDL	0 (0)	0 (0)	BDL
Elaeis guianensis	0 (0)	BDL	BDL	1.12 (0.06)	0 (0)	BDL
Inga spp.	0 (0)	BDL	BDL	0 (0)	0 (0)	BDL
Melia azedarach	0 (0)	BDL	0 (0)	0.46 (0.02)	0 (0)	BDL
Musa spp.	0 (0)	BDL	BDL	0 (0)	0 (0)	BDL
Pachira aquatica	0 (0)	0	BDL	1.61 (0.08)	0 (0)	BDL
Spathodea campanulata	0 (0)	BDL	BDL	0 (0)	0 (0)	BDL
Eucalyptus camaldulensis	0 (0)	BDL	0.29 (0.01)	9.6 (0.5)	0.089 (0.004)	1.22 (0.06)
Eucalyptus erythrocorys	0.19 (0.02)	0	0 (0)	2 (1)	0.032 (0.002)	0.0 (0.2)
Eucalyptus microtheca	0.06 (0.02)	BDL	0 (0)	1 (1)	0 (0)	0.0 (0.2)
Eucalyptus papuana	0.11 (0.02)	BDL	0.0038 (0.0001)	2 (1)	0 (0)	0.1 (0.2)
Eucalyptus woodwardii	0.22 (0.02)	BDL	0.084 (0.004)	45 (3)	0 (0)	0.0 (0.2)
Pascopyrum smithii	0.29 (0.02)	BDL	0 (0)	3 (1)	0.144 (0.007)	0.0 (0.2)
Elymus elymoides	0.49 (0.03)	BDL	0 (0)	3 (1)	0.36 (0.02)	0.2 (0.2)
Thinopyrum intermedium	0.52 (0.03)	0	0 (0)	5 (1)	0.71 (0.04)	0.4 (0.2)
Bouteloua gracilis	0.56 (0.04)	BDL	0 (0)	8 (1)	0.77 (0.04)	0.3 (0.2)
Sorghastrum nutans	0.35 (0.03)	BDL	0 (0)	1 (1)	0.43 (0.02)	0.1 (0.2)

APPENDIX G

DATA: TRACE METALS IN FINE AEROSOLS

Table 24: Fine fraction field blank aerosol concentrations of Na, Mg, Al, P, K, Ca, and Ti. The average filter blank concentration of each trace metal was subtracted from the field blanks.

Field Blank	Na (µg)	Mg (µg)	Al (µg)	P (µg)	K (µg)	Ca (µg)	Ti (µg)
1	0 (32)	4.2 (0.3)	3.3 (0.6)	0 (2)	0 (8)	1 (6)	0.27 (0.04)
2	0 (32)	6.2 (0.4)	11.6 (0.8)	5 (2)	14 (8)	14 (6)	0.54 (0.05)
3	5 (2)	2.7 (0.3)	12 (1)	1.3 (0.4)	5 (1)	2.1 (0.1)	0.6 (0.1)
4	1 (2)	1.4 (0.2)	15.8 (1.1)	0.1 (0.3)	3 (1)	BDL	1.1 (0.2)
5	1 (2)	0.7 (0.2)	1.8 (0.7)	0 (0.3)	2 (1)	BDL	0.1 (0.1)
6	7 (2)	1.5 (0.2)	3.4 (0.7)	0.7 (0.3)	4 (1)	BDL	0.3 (0.1)
7	1 (2)	2.6 (0.3)	3.3 (0.7)	0.3 (0.3)	10 (1)	1.9 (0.1)	0.2 (0.1)
8	0 (23)	3.4 (0.4)	2.7 (0.1)	0 (2)	17 (1)	12 (2)	0.3 (0.2)
9	6 (23)	1.2 (0.3)	0.19 (0.01)	0 (2)	4.8 (0.7)	0 (2)	0.2 (0.2)
10	0 (23)	1.1 (0.3)	2.7 (0.1)	0 (2)	2 (0.7)	6 (2)	0.2 (0.2)
11	0 (23)	3.6 (0.4)	7.1 (0.4)	0 (2)	4.1 (0.7)	5 (2)	0.7 (0.2)

Table 25: Fine fraction field blank aerosol concentrations of V, Cr, Mn, Co, Ni, and Cu. The average filter blank concentration of each trace metal was subtracted from the field blanks.

Field Blank	V (ng)	Cr (ng)	Mn (µg)	Co (ng)	Ni (ng)	Cu (µg)
1	7.2 (0.4)	51 (64)	0 (0.2)	6.6 (0.3)	12 (3)	4.2 (0.2)
2	17.2 (0.9)	1422 (97)	1.2 (0.2)	4848 (242)	137 (8)	3.3 (0.2)
3	8 (7)	51 (60)	0.16 (0.02)	4 (3)	20 (17)	BDL
4	9 (7)	503 (66)	0.07 (0.02)	4 (3)	30 (17)	BDL
5	5 (7)	18 (60)	0.02 (0.02)	2 (3)	10 (17)	BDL
6	7 (7)	3 (60)	0.04 (0.02)	1 (3)	0 (17)	BDL
7	1 (7)	0 (60)	0.05 (0.02)	0 (3)	0 (17)	BDL
8	9 (5)	53 (208)	0.19 (0.01)	0 (4)	25 (2)	0.94 (0.05)
9	0 (5)	0 (208)	0.058 (0.009)	0 (4)	6 (1)	0.55 (0.03)
10	10 (5)	62 (208)	0.056 (0.009)	1 (4)	3 (1)	0.46 (0.02)
11	16 (5)	64 (208)	0.19 (0.01)	0 (4)	28 (2)	0.85 (0.04)

Table 26: Fine fraction field blank aerosol concentrations of Zn, Rb, Sr, Zr, Mo, and Cd. The average filter blank concentration of each trace metal was subtracted from the field blanks.

Field Blank	Zn (μg)	Rb (ng)	Sr (ng)	Zr (ng)	Mo (ng)	Cd (ng)
1	0 (0.03)	3 (5)	5 (1)	18 (2)	4 (4)	2.8 (0.2)
2	0 (0.03)	19 (5)	40 (3)	21 (2)	2 (4)	2 (0.1)
3	2.3 (0.1)	18 (2)	42 (2)	21 (33)	0 (3)	0 (0)
4	0.45 (0.04)	11 (2)	42 (2)	33 (33)	4 (3)	0 (0)
5	0.37 (0.04)	3 (1)	BDL	0 (33)	3 (3)	0 (0)
6	0.36 (0.04)	4 (1)	10.6 (0.5)	24 (33)	1 (3)	0 (0)
7	0.27 (0.04)	5 (1)	25 (1)	4 (33)	1 (3)	0 (0)
8	3.6 (0.2)	10 (4)	109 (14)	18 (28)	0 (0)	0.5 (0.03)
9	0.4 (0.2)	11 (4)	2 (13)	0 (28)	0 (0)	0.132 (0.007)
10	0.1 (0.2)	5 (3)	38 (13)	0 (28)	0 (0)	0.29 (0.01)
11	0.3 (0.2)	12 (4)	35 (13)	0 (28)	0 (0)	0.91 (0.05)

Table 27: Fine fraction field blank aerosol concentrations of Cs, Ba, La, Ce, and Pr. The average filter blank concentration of each trace metal was subtracted from the field blanks.

Field Blank	Cs (ng)	Ba (μg)	La (ng)	Ce (ng)	Pr (ng)
1	0.56 (0.07)	0.12 (0.07)	2 (0.9)	6 (0.4)	0.4 (0.04)
2	1.6 (0.1)	0.13 (0.07)	6 (1)	11.6 (0.7)	1.4 (0.08)
3	1.6 (0.2)	0.07 (0.02)	5 (0.4)	10.1 (0.9)	1.1 (0.1)
4	0.7 (0.2)	0.06 (0.02)	9 (0.6)	19 (1)	1.9 (0.1)
5	0.2 (0.2)	0.05 (0.02)	1 (0.3)	2 (0.7)	0.19 (0.1)
6	0.3 (0.2)	0.06 (0.02)	1.6 (0.3)	3.3 (0.7)	0.35 (0.1)
7	0.4 (0.2)	0.04 (0.02)	1.4 (0.3)	3.1 (0.7)	0.24 (0.1)
8	0.5 (0.2)	24 (133)	0.75 (0.04)	1.56 (0.08)	0.25 (0.01)
9	0.4 (0.2)	125.5 (133.3)	0.57 (0.03)	1.33 (0.07)	0.107 (0.005)
10	0.3 (0.2)	13 (133)	0.41 (0.02)	1.44 (0.07)	0.29 (0.01)
11	0.8 (0.2)	326.2 (134.3)	2.6 (0.1)	5.8 (0.3)	0.65 (0.03)

Table 28: Fine fraction field blank aerosol concentrations of Nd, Sm, Eu, Gd, and Tb. The average filter blank concentration of each trace metal was subtracted from the field blanks.

Field Blank	Nd (ng)	Sm (ng)	Eu (ng)	Gd (ng)	Tb (ng)
1	1.5 (0.1)	0.2 (0.02)	0.08 (0.01)	0.3 (0.02)	BDL
2	5.3 (0.3)	1.16 (0.07)	0.21 (0.02)	0.9 (0.05)	0.158 (0.008)
3	4.5 (0.5)	0.82 (0.1)	0.17 (0.01)	0.76 (0.05)	0.115 (0.006)
4	6.3 (0.5)	1.4 (0.1)	0.23 (0.01)	1.03 (0.06)	0.17 (0.008)
5	0.7 (0.4)	0.1 (0.09)	0.023 (0.006)	0.12 (0.03)	0.026 (0.001)
6	1.5 (0.4)	0.31 (0.09)	0.067 (0.008)	0.29 (0.04)	0.046 (0.002)
7	1 (0.4)	0.28 (0.09)	0.046 (0.007)	0.18 (0.03)	0.039 (0.002)
8	0.7 (0.04)	0.3 (0.02)	0.093 (0.005)	0.23 (0.01)	0 (0.1)
9	0.62 (0.03)	0.059 (0.003)	0.052 (0.003)	0.159 (0.008)	0 (0.1)
10	0.96 (0.05)	0.4 (0.02)	0.065 (0.003)	0.3 (0.02)	0 (0.1)
11	2.5 (0.1)	0.49 (0.02)	0.141 (0.007)	0.51 (0.03)	0.1 (0.1)

Table 29: Fine fraction field blank aerosol concentrations of Dy, Ho, Er, Tm, and Yb. The average filter blank concentration of each trace metal was subtracted from the field blanks.

Field Blank	Dy (ng)	Ho (ng)	Er (ng)	Tm (ng)	Yb (ng)
1	0.22 (0.06)	0.024 (0.003)	0.12 (0.07)	0.011 (0.001)	0.08 (0.02)
2	0.77 (0.07)	0.141 (0.009)	0.44 (0.07)	0.054 (0.003)	0.38 (0.03)
3	0.7 (0.09)	0.159 (0.008)	0.4 (0.02)	0.061 (0.007)	0.47 (0.02)
4	1 (0.09)	0.23 (0.01)	0.62 (0.03)	0.078 (0.007)	0.74 (0.04)
5	0.08 (0.08)	0.031 (0.002)	0.135 (0.007)	0 (0.005)	0.127 (0.006)
6	0.21 (0.08)	0.066 (0.003)	0.23 (0.01)	0.004 (0.006)	0.2 (0.01)
7	0.15 (0.08)	0.042 (0.002)	0.114 (0.006)	0.001 (0.005)	0.145 (0.007)
8	0.25 (0.01)	0.048 (0.002)	0.137 (0.007)	0.021 (0.001)	0.103 (0.005)
9	0 (0)	0.03 (0.001)	0.067 (0.003)	0 (0)	0.077 (0.004)
10	0.148 (0.007)	0.052 (0.003)	0.112 (0.006)	0.011 (0.001)	0.071 (0.004)
11	0.4 (0.02)	0.071 (0.004)	0.26 (0.01)	0.039 (0.002)	0.26 (0.01)

Table 30: Fine fraction field blank aerosol concentrations of Lu, Hf, W, Re, Pb and U. The average filter blank concentration of each trace metal was subtracted from the field blanks.

Field Blank	Lu (ng)	Hf (ng)	W (ng)	Re (ng)	Pb (ng)	U (ng)
1	0.019 (0.003)	0.35 (0.09)	1 (3)	0.079 (0.004)	79 (4)	BDL
2	0.049 (0.004)	0.57 (0.09)	0 (3)	0.028 (0.001)	49 (3)	BDL
3	0.059 (0.003)	0.7 (0.7)	25 (1)	BDL	9.6 (0.7)	BDL
4	0.097 (0.005)	1.1 (0.8)	5 (0.4)	0 (0)	7.8 (0.7)	1.25 (0.06)
5	0.014 (0.001)	0 (0.7)	0 (0.2)	BDL	4.2 (0.6)	BDL
6	0.019 (0.001)	0.6 (0.7)	20 (1)	BDL	2.9 (0.5)	BDL
7	0.013 (0.001)	0.3 (0.7)	4.5 (0.4)	BDL	6.5 (0.6)	BDL
8	0.021 (0.002)	0.5 (0.6)	BDL	0 (0)	14 (1)	0.041 (0.002)
9	0.019 (0.002)	0 (0.6)	BDL	0 (0)	9.8 (0.9)	0 (0)
10	0.012 (0.002)	0.2 (0.6)	25 (1)	0 (0)	5.7 (0.7)	0.036 (0.002)
11	0.045 (0.003)	0 (0.6)	0 (0)	0 (0)	17 (1)	0.108 (0.005)

Table 31: Fine fraction burn aerosol concentrations of Na, Mg, AL, P, K, Ca, Ti, V, and Cr. The average filter blank concentration of each trace metal analyzed was subtracted from the aerosol samples.

Sample Name	Na (µg)	Mg (µg)	Al (µg)	P (µg)	K (mg)	Ca (µg)	Ti (µg)	V (ng)	Cr (ng)
Pinus ponderosa 1	0 (32)	2.3 (0.2)	1.4 (0.5)	10 (2)	4.1 (0.2)	1 (6)	0.03 (0.04)	0 (0)	1686 (108)
Pinus ponderosa 2	0 (32)	6.5 (0.4)	4.2 (0.6)	18 (2)	11.2 (0.6)	9 (6)	0.22 (0.04)	0.45 (0.02)	211 (65)
Pinus ponderosa 3	0 (32)	14.8 (0.8)	5.5 (0.6)	25 (2)	8.1 (0.4)	16 (6)	0.17 (0.04)	0.56 (0.03)	80 (64)
Pinus ponderosa 4	0 (32)	5.1 (0.4)	5 (0.6)	12 (2)	4.6 (0.2)	5 (6)	0.14 (0.04)	2.55 (0.13)	201 (65)
Arenga pinnata	34 (3)	9.2 (0.5)	12 (1)	3.7 (0.4)	1.19 (0.06)	22 (1)	0.7 (0.1)	14 (7)	58 (60)
Bambusa spp.	3 (2)	4.3 (0.3)	5.2 (0.8)	2.8 (0.4)	2.2 (0.1)	5.2 (0.3)	0.5 (0.1)	0 (7)	39 (60)
Cissus sicyoides	55 (4)	11.8 (0.6)	22 (1)	7.2 (0.6)	0.89 (0.04)	52 (3)	1.4 (0.2)	27 (8)	63 (60)
Costas spp.	4 (2)	8.2 (0.5)	11 (1)	2.4 (0.4)	1.02 (0.05)	40 (2)	0.7 (0.1)	2 (7)	58 (60)
Elaeis guianensis	44 (4)	9.1 (0.5)	15 (1)	10.6 (0.7)	2.3 (0.1)	15.3 (0.8)	1.6 (0.2)	17 (7)	463 (65)
Inga spp.	29 (3)	7.9 (0.5)	2.2 (0.7)	3.5 (0.4)	1.89 (0.09)	10 (0.5)	0.3 (0.1)	0 (7)	39 (60)
Melia azedarach	15 (3)	71 (4)	4.5 (0.8)	18 (1)	2.1 (0.1)	135 (7)	3.7 (0.2)	2 (7)	18 (60)
Musa spp.	4 (2)	5.7 (0.4)	12 (1)	2.3 (0.4)	3.2 (0.2)	12.6 (0.6)	0.9 (0.1)	0 (7)	416 (64)
Pachira aquatica	19 (3)	12 (0.7)	3.3 (0.7)	1.8 (0.4)	2.3 (0.1)	26 (1)	0.2 (0.1)	0 (7)	0 (60)
Spathodea campanulata	7 (2)	4.6 (0.3)	18 (1)	2.3 (0.4)	0.76 (0.04)	15 (0.8)	1.3 (0.2)	15 (7)	489 (66)
Eucalyptus camaldulensis	44 (4)	4.5 (0.3)	8.7 (0.9)	0.8 (0.3)	0.74 (0.04)	20 (1)	0.6 (0.1)	8 (7)	228 (61)
Eucalyptus erythrocorys	1957 (102)	16.7 (0.9)	0 (0)	8 (2)	3 (0.2)	13 (2)	0.1 (0.2)	0 (5)	16 (208)
Eucalyptus microtheca	289 (28)	5.1 (0.4)	7.9 (0.4)	2 (2)	3 (0.2)	7 (2)	0.6 (0.2)	0 (5)	0 (208)
Eucalyptus papuana	189 (26)	3.2 (0.4)	0.35 (0.02)	5 (2)	6.2 (0.3)	9 (2)	0.1 (0.2)	0 (5)	0 (208)
Eucalyptus woodwardii	3000 (153)	4.6 (0.4)	10 (0.5)	4 (2)	3.5 (0.2)	17 (2)	0.9 (0.2)	0 (5)	130 (208)
Pascopyrum smithii	25 (23)	7.8 (0.5)	18.3 (0.9)	7 (2)	0.24 (0.01)	16 (2)	1.7 (0.2)	22 (5)	0 (208)
Elymus elymoides	21 (23)	14.6 (0.8)	52 (3)	9 (2)	1.05 (0.05)	30 (2)	4.5 (0.3)	60 (6)	0 (208)
Thinopyrum intermedium	0 (23)	9.6 (0.6)	13.3 (0.7)	10 (2)	3.2 (0.2)	19 (2)	1.1 (0.2)	11 (5)	104 (208)
Bouteloua gracilis	52 (24)	42 (2)	124 (6)	26 (3)	1.33 (0.07)	91 (5)	11.1 (0.6)	235 (13)	460 (210)
Sorghastrum nutans	0 (23)	16.3 (0.9)	26 (1)	12 (2)	1.21 (0.06)	24 (2)	2.4 (0.2)	35 (5)	37 (208)

Table 32: Fine fraction burn aerosol concentrations of Mn, Co, Ni, Cu, Zn, Rb, Sr, Zr, and Mo. The average filter blank concentration of each trace metal analyzed was subtracted from the aerosol samples.

Sample Name	Mn (µg)	Co (ng)	Ni (ng)	Cu (µg)	Zn (µg)	Rb (µg)	Sr (ng)	Zr (ng)	Mo (ng)
Pinus ponderosa 1	1.4 (0.2)	3.9 (0.8)	7752 (388)	203 (11)	2.7 (0.1)	2.02 (0.1)	0 (0.9)	7 (2)	5 (4)
Pinus ponderosa 2	3.3 (0.3)	5.7 (0.9)	315 (16)	88 (6)	4.9 (0.2)	5.4 (0.3)	7 (1)	6 (2)	3 (4)
Pinus ponderosa 3	4.8 (0.3)	6.2 (0.9)	103 (5)	53 (4)	4.9 (0.2)	4.1 (0.2)	15 (2)	8 (2)	5 (4)
Pinus ponderosa 4	1.8 (0.2)	5.5 (0.9)	891 (45)	60 (5)	3.2 (0.2)	2.8 (0.1)	2 (1)	38 (3)	1 (4)
Arenga pinnata	0.54 (0.03)	14 (2)	6 (3)	20 (17)	1.26 (0.06)	0.12 (0.01)	113 (6)	35 (33)	7 (3)
Bambusa spp.	0.41 (0.03)	11 (2)	3 (3)	26 (17)	2.09 (0.1)	0.66 (0.03)	31 (2)	3 (33)	10 (3)
Cissus sicyoides	0.42 (0.03)	14 (2)	7 (3)	22 (17)	1.17 (0.06)	0.17 (0.01)	239 (12)	17 (33)	26 (3)
Costas spp.	2.4 (0.1)	7 (2)	5 (3)	26 (17)	BDL	0.41 (0.02)	122 (6)	0 (33)	9 (3)
Elaeis guianensis	1.19 (0.06)	6 (2)	6 (3)	16 (17)	0.5 (0.03)	0.53 (0.03)	69 (3)	59 (33)	17 (3)
Inga spp.	1.57 (0.08)	6 (2)	13 (3)	27 (17)	1.57 (0.08)	1.04 (0.05)	50 (3)	11 (33)	25 (3)
Melia azedarach	1.02 (0.05)	4 (2)	26 (3)	13 (17)	BDL	0.43 (0.02)	653 (33)	31 (33)	31 (3)
Musa spp.	2.8 (0.1)	5 (2)	2 (3)	2 (17)	0.62 (0.03)	0.11 (0.01)	69 (3)	23 (33)	11 (3)
Pachira aquatica	2.4 (0.1)	26 (2)	15 (3)	20 (17)	0.98 (0.05)	0.28 (0.01)	142 (7)	22 (33)	5 (3)
Spathodea campanulata	0.1 (0.02)	3 (2)	1 (3)	0 (17)	BDL	0.27 (0.01)	94 (5)	49 (33)	4 (3)
Eucalyptus camaldulensis	0.17 (0.02)	2 (2)	0 (3)	6 (17)	BDL	0.11 (0.01)	156 (8)	17 (33)	2 (3)
Eucalyptus erythrocorys	0.17 (0.01)	11 (1)	0 (4)	23 (2)	1.24 (0.06)	0.56 (0.03)	113 (14)	0 (28)	0 (0)
Eucalyptus microtheca	0.23 (0.01)	4.6 (0.9)	2 (4)	16 (1)	0.42 (0.02)	0.39 (0.02)	90 (14)	0 (28)	0 (0)
Eucalyptus papuana	0.48 (0.03)	2.4 (0.9)	350 (18)	115 (6)	3.8 (0.2)	3.2 (0.2)	77 (14)	0 (28)	0 (0)
Eucalyptus woodwardii	0.47 (0.03)	4.7 (0.9)	6 (4)	59 (3)	1.27 (0.06)	1.27 (0.06)	151 (15)	42 (28)	0 (0)
Pascopyrum smithii	0.33 (0.02)	13 (1)	6 (4)	46 (3)	0.45 (0.02)	0.15 (0.01)	150 (15)	73 (29)	0 (0)
Elymus elymoides	0.88 (0.05)	37 (2)	12 (4)	28 (2)	0.59 (0.03)	0.93 (0.05)	342 (22)	68 (28)	0 (0)
Thinopyrum intermedium	0.76 (0.04)	9.8 (1)	3 (4)	14 (1)	0.62 (0.03)	3.2 (0.2)	162 (16)	0 (28)	0 (0)
Bouteloua gracilis	1.9 (0.1)	94 (5)	31 (4)	119 (6)	0.69 (0.04)	1.29 (0.06)	1057 (55)	252 (32)	0 (0)
Sorghastrum nutans	0.71 (0.04)	22 (1)	4 (4)	44 (3)	0.4 (0.02)	1.17 (0.06)	250 (18)	47 (28)	0 (0)

Table 33: Fine fraction burn aerosol concentrations of Cd, Cs, Ba, La, Ce, Pr, Nd, and Sm. The average filter blank concentration of each trace metal analyzed was subtracted from the aerosol samples.

Sample Name	Cd (ng)	Cs (ng)	Ba (μg)	La (ng)	Ce (ng)	Pr (ng)	Nd (ng)	Sm (ng)
Pinus ponderosa 1	457 (23)	10.7 (0.5)	0.01 (0.07)	0.8 (0.9)	1.6 (0.2)	0.2 (0.04)	0.76 (0.09)	0.12 (0.02)
Pinus ponderosa 2	1156 (58)	21 (1)	0.14 (0.07)	2 (0.9)	3.8 (0.3)	0.48 (0.04)	2.1 (0.1)	0.32 (0.03)
Pinus ponderosa 3	1074 (54)	24 (1)	0.03 (0.07)	3.7 (0.9)	6.6 (0.5)	0.77 (0.06)	2.8 (0.2)	0.5 (0.04)
Pinus ponderosa 4	478 (24)	14.5 (0.7)	0.03 (0.07)	2.3 (0.9)	4.2 (0.3)	0.53 (0.05)	2 (0.1)	0.46 (0.03)
Arenga pinnata	274 (14)	2 (0.2)	0.15 (0.02)	3.5 (0.4)	7.3 (0.8)	0.8 (0.1)	3.1 (0.4)	0.7 (0.1)
Bambusa spp.	8.2 (0.4)	1.3 (0.2)	0.05 (0.02)	1.5 (0.3)	3 (0.7)	0.3 (0.1)	1.2 (0.4)	0.34 (0.09)
Cissus sicyoides	1.17 (0.06)	3.9 (0.3)	0.26 (0.03)	9 (0.6)	18 (1)	2 (0.1)	8.1 (0.6)	1.6 (0.1)
Costas spp.	11.1 (0.6)	3.1 (0.2)	0.17 (0.02)	3.5 (0.4)	7 (0.8)	0.8 (0.1)	3.1 (0.4)	0.6 (0.1)
Elaeis guianensis	30 (2)	21 (1)	0.06 (0.02)	11.9 (0.7)	25 (1)	2.2 (0.2)	8.1 (0.6)	1.3 (0.1)
Inga spp.	52 (3)	49 (2)	0.03 (0.02)	0.8 (0.3)	1.8 (0.7)	0.12 (0.1)	0.5 (0.4)	0.16 (0.09)
Melia azedarach	4.6 (0.2)	5 (0.3)	1.43 (0.08)	1.5 (0.3)	3 (0.7)	0.3 (0.1)	1.2 (0.4)	0.39 (0.09)
Musa spp.	2.2 (0.1)	0.8 (0.2)	0.09 (0.02)	5.6 (0.4)	12 (1)	1.1 (0.1)	3.7 (0.5)	0.72 (0.1)
Pachira aquatica	32 (2)	1 (0.2)	0.09 (0.02)	0.8 (0.3)	1.7 (0.7)	0.2 (0.1)	0.5 (0.4)	0.21 (0.09)
Spathodea campanulata	2.4 (0.1)	4.1 (0.3)	0.11 (0.02)	11.8 (0.7)	25 (1)	2.4 (0.2)	9.2 (0.6)	1.7 (0.1)
Eucalyptus camaldulensis	40 (2)	5 (0.3)	0.06 (0.02)	3.1 (0.4)	6.1 (0.8)	0.6 (0.1)	2.3 (0.4)	0.48 (0.09)
Eucalyptus erythrocorys	23 (1)	5 (0.3)	0 (0.1)	0.69 (0.03)	0.8 (0)	0.13 (0.01)	0.3 (0)	0.17 (0.01)
Eucalyptus microtheca	55 (3)	4.5 (0.3)	0.1 (0.1)	7.8 (0.4)	15.9 (0.8)	1.5 (0.07)	5.8 (0.3)	0.93 (0.05)
Eucalyptus papuana	597 (30)	20 (1)	0.1 (0.1)	0 (0)	0 (0)	0 (0)	0 (0)	0 (0)
Eucalyptus woodwardii	357 (18)	24 (1)	0.1 (0.1)	5.5 (0.3)	12.6 (0.6)	1.15 (0.06)	4.5 (0.2)	0.76 (0.04)
Pascopyrum smithii	78 (4)	2.8 (0.2)	0.3 (0.1)	8.2 (0.4)	17 (0.9)	1.73 (0.09)	7.3 (0.4)	1.49 (0.07)
Elymus elymoides	75 (4)	8.8 (0.5)	0.5 (0.1)	27 (1)	51 (3)	5.6 (0.3)	22 (1)	4.2 (0.2)
Thinopyrum intermedium	13.8 (0.7)	8.3 (0.4)	0.2 (0.1)	6 (0.3)	11.7 (0.6)	1.38 (0.07)	5.7 (0.3)	1.28 (0.06)
Bouteloua gracilis	135 (7)	7.6 (0.4)	1.5 (0.2)	57 (3)	109 (5)	12.07 (0.6)	49 (2)	9.1 (0.5)
Sorghastrum nutans	77 (4)	3.8 (0.3)	0.4 (0.1)	11.4 (0.6)	22 (1)	2.5 (0.1)	9.7 (0.5)	1.91 (0.1)

Table 34: Fine fraction burn aerosol concentrations of Eu, Gd, Tb, Dy, Ho, Er, and Tm. The average filter blank concentration of each trace metal analyzed was subtracted from the aerosol samples.

Sample Name	Eu (ng)	Gd (ng)	Tb (ng)	Dy (ng)	Ho (ng)	Er (ng)	Tm (ng)
Pinus ponderosa 1	0.02 (0.01)	0.12 (0.01)	0.05 (0)	0.15 (0.05)	0.022 (0.003)	0.09 (0.07)	0.01 (0)
Pinus ponderosa 2	0.12 (0.01)	0.31 (0.02)	0.07 (0)	0.27 (0.06)	0.052 (0.004)	0.15 (0.07)	0.03 (0)
Pinus ponderosa 3	0.08 (0.01)	0.42 (0.03)	0.07 (0)	0.34 (0.06)	0.045 (0.004)	0.18 (0.07)	0.02 (0)
Pinus ponderosa 4	0.08 (0.01)	0.33 (0.02)	0.08 (0)	0.43 (0.06)	0.08 (0.01)	0.23 (0.07)	0.02 (0)
Arenga pinnata	0.15 (0.01)	0.55 (0.04)	0.1 (0)	0.51 (0.08)	0.12 (0.01)	0.39 (0.02)	0.03 (0.01)
Bambusa spp.	0.07 (0.01)	0.31 (0.04)	0.06 (0)	0.21 (0.08)	0.063 (0.003)	0.2 (0.01)	0.02 (0.01)
Cissus sicyoides	0.33 (0.02)	1.55 (0.09)	0.22 (0.01)	1.5 (0.1)	0.33 (0.02)	0.91 (0.05)	0.12 (0.01)
Costas spp.	0.17 (0.01)	0.59 (0.05)	0.11 (0.01)	0.64 (0.08)	0.15 (0.01)	0.4 (0.02)	0.04 (0.01)
Elaeis guianensis	0.26 (0.02)	1.2 (0.07)	0.18 (0.01)	1.02 (0.09)	0.23 (0.01)	0.67 (0.03)	0.08 (0.01)
Inga spp.	0.05 (0.01)	0.18 (0.03)	0.05 (0)	0.18 (0.08)	0.046 (0.002)	0.15 (0.01)	0.02 (0.01)
Melia azedarach	0.09 (0.01)	0.24 (0.03)	0.05 (0)	0.21 (0.08)	0.075 (0.004)	0.17 (0.01)	0 (0.01)
Musa spp.	0.13 (0.01)	0.66 (0.05)	0.11 (0.01)	0.55 (0.08)	0.14 (0.01)	0.41 (0.02)	0.04 (0.01)
Pachira aquatica	0.04 (0.01)	0.13 (0.03)	0.04 (0)	0.2 (0.08)	0.075 (0.004)	0.22 (0.01)	0.02 (0.01)
Spathodea campanulata	0.32 (0.02)	1.41 (0.08)	0.24 (0.01)	1.5 (0.1)	0.31 (0.02)	0.81 (0.04)	0.1 (0.01)
Eucalyptus camaldulensis	0.1 (0.01)	0.43 (0.04)	0.08 (0)	0.35 (0.08)	0.11 (0.01)	0.33 (0.02)	0.04 (0.01)
Eucalyptus erythrocorys	0.046 (0.002)	0.25 (0.01)	0.06 (0.1)	0.16 (0.01)	0.046 (0.002)	0.19 (0.01)	0.02 (0)
Eucalyptus microtheca	0.15 (0.01)	0.9 (0.04)	0.13 (0.1)	0.65 (0.03)	0.087 (0.004)	0.38 (0.02)	0.04 (0)
Eucalyptus papuana	0 (0)	0 (0)	0 (0.1)	0 (0)	0 (0)	0 (0)	0 (0)
Eucalyptus woodwardii	0.17 (0.01)	0.65 (0.03)	0.09 (0.1)	0.66 (0.03)	0.15 (0.01)	0.45 (0.02)	0.06 (0)
Pascopyrum smithii	0.34 (0.02)	1.16 (0.06)	0.15 (0.1)	1.11 (0.06)	0.23 (0.01)	0.59 (0.03)	0.08 (0)
Elymus elymoides	1.06 (0.05)	3.4 (0.2)	0.5 (0.1)	2.9 (0.1)	0.57 (0.03)	1.63 (0.08)	0.23 (0.01)
Thinopyrum intermedium	0.32 (0.02)	0.91 (0.05)	0.11 (0.1)	0.58 (0.03)	0.13 (0.01)	0.4 (0.02)	0.02 (0)
Bouteloua gracilis	2.6 (0.1)	7.7 (0.4)	1.2 (0.1)	6.7 (0.3)	1.32 (0.07)	3.9 (0.2)	0.52 (0.03)
Sorghastrum nutans	0.55 (0.03)	1.56 (0.08)	0.2 (0.1)	1.61 (0.08)	0.28 (0.01)	0.88 (0.04)	0.11 (0.01)

Table 35: Fine fraction burn aerosol concentrations of Yb, Lu, Hf, W, Re, Pb, and U. The average filter blank concentration of each trace metal analyzed was subtracted from the aerosol samples.

Sample Name	Yb (ng)	Lu (ng)	Hf (ng)	W (ng)	Re (ng)	Pb (ng)	U (ng)
Pinus ponderosa 1	0.09 (0.02)	0.01 (0.003)	0.11 (0.08)	0 (3)	1.46 (0.07)	111 (6)	BDL
Pinus ponderosa 2	0.16 (0.02)	0.015 (0.003)	0.15 (0.08)	0 (3)	6 (0.3)	166 (9)	BDL
Pinus ponderosa 3	0.21 (0.02)	0.022 (0.003)	0.27 (0.08)	0 (3)	4.8 (0.2)	198 (10)	BDL
Pinus ponderosa 4	0.2 (0.02)	0.015 (0.003)	0.9 (0.1)	3 (3)	2 (0.1)	98 (5)	BDL
Arenga pinnata	0.39 (0.02)	0.044 (0.003)	0.9 (0.8)	0 (0.2)	0.55 (0.03)	58 (3)	1.17 (0.06)
Bambusa spp.	0.21 (0.01)	0.014 (0.001)	0.1 (0.7)	2.6 (0.3)	0.45 (0.02)	11 (1)	BDL
Cissus sicyoides	0.82 (0.04)	0.1 (0.01)	0.5 (0.7)	8.9 (0.6)	0 (0)	38 (2)	0.78 (0.04)
Costas spp.	0.39 (0.02)	0.044 (0.003)	0.1 (0.7)	0 (0.2)	0 (0)	23 (1)	0.6 (0.03)
Elaeis guianensis	0.67 (0.03)	0.082 (0.005)	1.8 (0.8)	23 (1)	0 (0)	30 (2)	1.37 (0.07)
Inga spp.	0.16 (0.01)	0.015 (0.001)	0.4 (0.7)	2.2 (0.3)	0.02 (0)	21 (1)	BDL
Melia azedarach	0.19 (0.01)	0.014 (0.001)	0.9 (0.8)	3.3 (0.4)	0.45 (0.02)	46 (2)	0.53 (0.03)
Musa spp.	0.42 (0.02)	0.054 (0.003)	0.8 (0.8)	22 (1)	0.34 (0.02)	33 (2)	1.2 (0.06)
Pachira aquatica	0.21 (0.01)	0.023 (0.002)	0.6 (0.7)	0 (0.1)	0.04 (0)	184 (9)	BDL
Spathodea campanulata	0.81 (0.04)	0.1 (0.01)	1.4 (0.8)	26 (1)	0 (0)	29 (2)	1.25 (0.06)
Eucalyptus camaldulensis	0.28 (0.01)	0.053 (0.003)	0.5 (0.7)	1.4 (0.3)	1.85 (0.09)	77 (4)	0.48 (0.02)
Eucalyptus erythrocorys	0.15 (0.01)	0.028 (0.003)	0 (0.6)	BDL	3.2 (0.2)	210 (11)	0.07 (0)
Eucalyptus microtheca	0.24 (0.01)	0.039 (0.003)	0.2 (0.6)	0 (0)	5.9 (0.3)	178 (9)	0.12 (0.01)
Eucalyptus papuana	0.01 (0)	0.002 (0.002)	0 (0.6)	0 (0)	16.5 (0.8)	246 (12)	0 (0)
Eucalyptus woodwardii	0.47 (0.02)	0.062 (0.004)	1.1 (0.6)	18.8 (0.9)	14.6 (0.7)	525 (26)	0.62 (0.03)
Pascopyrum smithii	0.53 (0.03)	0.09 (0.01)	1.6 (0.6)	BDL	0.1 (0)	244 (12)	0.38 (0.02)
Elymus elymoides	1.53 (0.08)	0.22 (0.01)	1.8 (0.6)	0 (0)	0.56 (0.03)	163 (8)	1.25 (0.06)
Thinopyrum intermedium	0.26 (0.01)	0.039 (0.003)	0 (0.6)	BDL	2.2 (0.1)	65 (3)	0.11 (0.01)
Bouteloua gracilis	3.4 (0.2)	0.49 (0.02)	5.8 (0.7)	0 (0)	0.13 (0.01)	501 (25)	2.73 (0.14)
Sorghastrum nutans	0.68 (0.03)	0.13 (0.01)	1.2 (0.6)	0 (0)	0.1 (0.01)	94 (5)	0.45 (0.02)

APPENDIX H

DATA: TRACE METALS IN ASH

Table 36: Ash concentrations of Na, Mg, Al. P, K, Ca, Ti, and V. The reagent blank concentration of each trace metal analyzed was subtracted from the ash samples. *Costas spp.* and *Eucalyptus erythrocorys* were lost during sample processing.

Sample Name	Na (mg)	Mg (mg)	Al (mg)	P (mg)	K (mg)	Ca (mg)	Ti (µg)	V (µg)
Pinus ponderosa 1	1.04 (0.05)	69 (3)	18.5 (0.9)	139 (7)	558 (28)	88 (4)	526 (26)	10.1 (0.5)
Pinus ponderosa 2	2 (0.1)	99 (5)	27 (1)	245 (12)	1148 (57)	194 (10)	899 (45)	16.6 (0.8)
Pinus ponderosa 3	1.41 (0.07)	111 (6)	24 (1)	170 (8)	611 (31)	170 (9)	657 (33)	12.5 (0.6)
Pinus ponderosa 4	1.43 (0.07)	111 (6)	27 (1)	228 (11)	938 (47)	141 (7)	707 (35)	14.1 (0.7)
Arenga pinnata	31 (2)	58 (3)	0.98 (0.05)	60 (3)	535 (27)	565 (28)	243 (12)	0 (0)
Bambusa spp.	1.5 (0.08)	58 (3)	0.37 (0.02)	70 (4)	622 (31)	247 (12)	142 (7)	0 (0)
Cissus sicyoides	8.5 (0.4)	73 (4)	0.151 (0.008)	54 (3)	214 (11)	948 (47)	80 (4)	224 (11)
Costas spp.	0.23 (0.01)	2.3 (0.1)	0.76 (0.04)	1.27 (0.06)	18 (0.9)	11.02 (0.55)	44 (2)	0 (0)
Elaeis guianensis	29 (1)	166 (8)	0.49 (0.02)	70 (4)	580 (29)	724 (36)	155 (8)	0 (0)
Inga spp.	7.4 (0.4)	63 (3)	1.72 (0.09)	48 (2)	222 (11)	368 (18)	168 (8)	0 (0)
Melia azedarach	7.3 (0.4)	396 (20)	0.53 (0.03)	113 (6)	551 (28)	1290 (64)	522 (26)	0 (0)
Musa spp.	4 (0.2)	59 (3)	0.32 (0.02)	49 (2)	937 (47)	426 (21)	123 (6)	0 (0)
Pachira aquatica	7.9 (0.4)	104 (5)	1.01 (0.05)	62 (3)	499 (25)	950 (48)	634 (32)	821 (41)
Spathodea campanulata	2.2 (0.1)	66 (3)	0.72 (0.04)	48 (2)	334 (17)	352 (18)	110 (6)	0 (0)
Eucalyptus camaldulensis	60 (3)	286 (14)	11.12 (0.56)	101 (5)	590 (30)	1678 (84)	713 (36)	0 (0)
Eucalyptus microtheca	325 (16)	284 (14)	14.32 (0.72)	92 (5)	2084 (104)	1871 (94)	1289 (64)	0 (0)
Eucalyptus papuana	25 (1)	126 (6)	2 (0.1)	56 (3)	420 (21)	619 (31)	202 (10)	0 (0)
Eucalyptus woodwardii	97 (5)	50 (3)	1.08 (0.05)	17 (0.9)	324 (16)	223 (11)	103 (5)	0 (0)
Pascopyrum smithii	3.4 (0.2)	27 (1)	25 (1)	14.9 (0.7)	42 (2)	67 (3)	2321 (116)	0 (0)
Elymus elymoides	6.7 (0.3)	48 (2)	41 (2)	50 (2)	263 (13)	205 (10)	3730 (187)	0 (0)
Thinopyrum intermedium	1.9 (0.1)	28 (1)	9 (0.4)	40 (2)	237 (12)	65 (3)	841 (42)	0 (0)
Bouteloua gracilis	6.2 (0.3)	12.6 (0.6)	32 (2)	8 (0.4)	15.02 (0.75)	43 (2)	3197 (160)	0 (0)
Sorghastrum nutans	4.9 (0.2)	52 (3)	23 (1)	56 (3)	228 (11)	97 (5)	2060 (103)	0 (0)

Table 37: Ash concentrations of Cr, Mn, Co, Ni, Cu, Zn, Rb, Sr, and Zr. The reagent blank concentration of each trace metal analyzed was subtracted from the ash samples. *Costas spp.* and *Eucalyptus erythrocorys* were lost during sample processing.

Sample Name	Cr (µg)	Mn (mg)	Co (µg)	Ni (µg)	Cu (µg)	Zn (mg)	Rb (µg)	Sr (mg)	Zr (µg)
Pinus ponderosa 1	24 (1)	11.8 (0.6)	47 (2)	84 (4)	630 (32)	2 (0.1)	185 (9)	0.075 (0.004)	9.8 (0.5)
Pinus ponderosa 2	16 (0.8)	26 (1)	21 (1)	180 (9)	940 (47)	4.4 (0.2)	344 (17)	0.139 (0.007)	17 (0.9)
Pinus ponderosa 3	10.7 (0.5)	18.1 (0.9)	24 (1)	80 (4)	665 (33)	2.4 (0.1)	188 (9)	0.182 (0.009)	12.9 (0.6)
Pinus ponderosa 4	11 (0.5)	18.1 (0.9)	27 (1)	130 (6)	967 (48)	3 (0.2)	311 (16)	0.119 (0.006)	13.6 (0.7)
Arenga pinnata	47 (2)	0.72 (0.04)	BDL	BDL	271 (14)	0.58 (0.03)	43 (2)	1.24 (0.06)	9.9 (0.5)
Bambusa spp.	0 (0)	0.59 (0.03)	BDL	BDL	280 (14)	0.56 (0.03)	143 (7)	0.47 (0.02)	1.6 (0.08)
Cissus sicyoides	BDL	0.56 (0.03)	BDL	BDL	152 (8)	0.2 (0.01)	36 (2)	3.1 (0.2)	4.3 (0.2)
Costas spp.	0.03 (0)	0.17 (0.01)	BDL	BDL	4.7 (0.2)	0.015 (0.001)	5.1 (0.3)	0.033 (0.002)	0.43 (0.02)
Elaeis guianensis	0 (0)	3.3 (0.2)	BDL	0.04 (0)	186 (9)	1.18 (0.06)	107 (5)	0.93 (0.05)	3.7 (0.2)
Inga spp.	0 (0)	1.75 (0.09)	BDL	3.9 (0.2)	193 (10)	0.54 (0.03)	104 (5)	1.12 (0.06)	2.2 (0.1)
Melia azedarach	0 (0)	2.9 (0.1)	37 (2)	15.3 (0.8)	143 (7)	0.58 (0.03)	97 (5)	4.7 (0.2)	9.7 (0.5)
Musa spp.	BDL	4.4 (0.2)	BDL	2.1 (0.1)	134 (7)	0.5 (0.03)	24 (1)	1.27 (0.06)	0 (0)
Pachira aquatica	BDL	2.2 (0.1)	BDL	BDL	183 (9)	0.4 (0.02)	48 (2)	4.2 (0.2)	9.2 (0.5)
Spathodea campanulata	0 (0)	0.37 (0.02)	BDL	6.1 (0.3)	204 (10)	0.32 (0.02)	108 (5)	0.87 (0.04)	2.3 (0.1)
Eucalyptus camaldulensis	6.1 (0.3)	10.4 (0.5)	BDL	146 (7)	356 (18)	4.3 (0.2)	67 (3)	11.2 (0.6)	15.4 (0.8)
Eucalyptus microtheca	14.5 (0.7)	8.6 (0.4)	BDL	99 (5)	328 (16)	1.9 (0.1)	231 (12)	16.1 (0.8)	32 (2)
Eucalyptus papuana	2 (0.1)	7.4 (0.4)	287 (14)	162 (8)	511 (26)	2.3 (0.1)	172 (9)	4.6 (0.2)	6.4 (0.3)
Eucalyptus woodwardii	162 (8)	1.15 (0.06)	418 (21)	19 (1)	72 (4)	0.4 (0.02)	54 (3)	2 (0.1)	6.3 (0.3)
Pascopyrum smithii	37 (2)	0.82 (0.04)	BDL	28 (1)	132 (7)	0.3 (0.01)	44 (2)	0.55 (0.03)	44 (2)
Elymus elymoides	42 (2)	2.4 (0.1)	BDL	13.3 (0.7)	116 (6)	0.53 (0.03)	231 (12)	1.14 (0.06)	72 (4)
Thinopyrum intermedium	3.4 (0.2)	1.58 (0.08)	BDL	4.8 (0.2)	91 (5)	0.38 (0.02)	211 (11)	0.44 (0.02)	17.8 (0.9)
Bouteloua gracilis	22 (1)	0.67 (0.03)	BDL	12.3 (0.6)	66 (3)	0.26 (0.01)	22 (1)	0.44 (0.02)	57 (3)
Sorghastrum nutans	15.5 (0.8)	1.9 (0.1)	BDL	50 (2)	149 (7)	0.74 (0.04)	236 (12)	0.67 (0.03)	46 (2)

Table 38: Ash concentrations of Mo, Cd, Cs, Ba, La, Ce, Pr, and Nd. The reagent blank concentration of each trace metal analyzed was subtracted from the ash samples. *Costas spp.* and *Eucalyptus erythrocorys* were lost during sample processing.

Sample Name	Mo (µg)	Cd (µg)	Cs (ng)	Ba (µg)	La (µg)	Ce (µg)	Pr (ng)	Nd (µg)
Pinus ponderosa 1	7.1 (0.4)	2.5 (0.1)	1053 (53)	86 (4)	5.1 (0.3)	9.5 (0.5)	1134 (57)	4.7 (0.2)
Pinus ponderosa 2	6 (0.3)	2.3 (0.1)	1490 (75)	151 (8)	9.7 (0.5)	17.5 (0.9)	2145 (107)	9 (0.4)
Pinus ponderosa 3	7.1 (0.4)	1.59 (0.08)	1288 (64)	142 (7)	8.4 (0.4)	15.4 (0.8)	1909 (95)	7.9 (0.4)
Pinus ponderosa 4	9.5 (0.5)	2.2 (0.1)	1539 (77)	121 (6)	8 (0.4)	14.8 (0.7)	1770 (89)	7.2 (0.4)
Arenga pinnata	21 (1)	1.04 (0.05)	448 (22)	614 (31)	0.53 (0.03)	0.83 (0.04)	109 (5)	0.51 (0.03)
Bambusa spp.	81 (4)	0.12 (0.01)	178 (9)	859 (43)	0.129 (0.006)	0.21 (0.01)	24 (1)	0.095 (0.005)
Cissus sicyoides	282 (14)	0.3 (0.02)	515 (26)	1342 (67)	0.53 (0.03)	0.72 (0.04)	73 (4)	0.265 (0.013)
Costas spp.	2.7 (0.1)	0.02 (0)	81 (4)	49 (2)	0.34 (0.02)	0.66 (0.03)	74 (4)	0.292 (0.015)
Elaeis guianensis	95 (5)	0.16 (0.01)	3426 (171)	295 (15)	0.3 (0.02)	0.54 (0.03)	62 (3)	0.271 (0.014)
Inga spp.	144 (7)	0.24 (0.01)	5022 (251)	404 (20)	0.89 (0.04)	1.7 (0.08)	209 (10)	0.84 (0.04)
Melia azedarach	125 (6)	0.29 (0.01)	982 (49)	2466 (123)	1.62 (0.08)	2.5 (0.1)	253 (13)	1.04 (0.05)
Musa spp.	92 (5)	0.12 (0.01)	85 (4)	865 (43)	0.131 (0.007)	0.33 (0.02)	25 (1)	0.125 (0.006)
Pachira aquatica	7.7 (0.4)	BDL	BDL	1234 (62)	1.5 (0.07)	3.1 (0.2)	233 (12)	1.02 (0.05)
Spathodea campanulata	24 (1)	0.19 (0.01)	1430 (71)	600 (30)	0.73 (0.04)	1.4 (0.07)	156 (8)	0.64 (0.03)
Eucalyptus camaldulensis	8.2 (0.4)	0.15 (0.01)	2348 (117)	2616 (131)	15 (0.8)	31 (2)	3089 (154)	12.1 (0.6)
Eucalyptus microtheca	10.5 (0.5)	0.6 (0.03)	1797 (90)	1027 (51)	13.8 (0.7)	28 (1)	2992 (150)	11.5 (0.6)
Eucalyptus papuana	9.8 (0.5)	0.34 (0.02)	1004 (50)	1060 (53)	2.5 (0.1)	4.8 (0.2)	521 (26)	2 (0.1)
Eucalyptus woodwardii	2.9 (0.1)	0.23 (0.01)	295 (15)	138 (7)	0.91 (0.05)	1.81 (0.09)	183 (9)	0.77 (0.04)
Pascopyrum smithii	39 (2)	0.2 (0.01)	1749 (87)	794 (40)	20 (1)	39 (2)	4269 (213)	16.7 (0.8)
Elymus elymoides	68 (3)	0.36 (0.02)	2725 (136)	1268 (63)	26 (1)	52 (3)	5398 (270)	21 (1)
Thinopyrum intermedium	14.3 (0.7)	0.08 (0)	715 (36)	486 (24)	5.8 (0.3)	10.9 (0.5)	1185 (59)	4.7 (0.2)
Bouteloua gracilis	5.5 (0.3)	0.18 (0.01)	1358 (68)	875 (44)	25 (1)	47 (2)	5111 (256)	20 (1)
Sorghastrum nutans	11.4 (0.6)	0.37 (0.02)	1513 (76)	1183 (59)	15.4 (0.8)	29 (1)	3131 (157)	12.3 (0.6)

Table 39: Ash concentrations of Sm, Eu, Gd, Tb, Dy, Ho, Er, and Tm. The reagent blank concentration of each trace metal analyzed was subtracted from the ash samples. *Costas spp.* and *Eucalyptus erythrocorys* were lost during sample processing.

Sample Name	Sm (ng)	Eu (ng)	Gd (ng)	Tb (ng)	Dy (ng)	Ho (ng)	Er (ng)	Tm (ng)
Pinus ponderosa 1	902 (45)	203 (10)	849 (42)	137 (7)	860 (43)	176 (9)	505 (25)	67 (3)
Pinus ponderosa 2	1781 (89)	387 (19)	1731 (87)	280 (14)	1728 (86)	373 (19)	1054 (53)	132 (7)
Pinus ponderosa 3	1539 (77)	322 (16)	1359 (68)	211 (11)	1265 (63)	258 (13)	726 (36)	93 (5)
Pinus ponderosa 4	1396 (70)	305 (15)	1256 (63)	200 (10)	1213 (61)	250 (12)	710 (35)	93 (5)
Arenga pinnata	110 (6)	97 (5)	105 (5)	17.5 (0.9)	102 (5)	26 (1)	70 (4)	8.3 (0.4)
Bambusa spp.	25 (1)	114 (6)	21 (1)	BDL	16.3 (0.8)	BDL	9.3 (0.5)	BDL
Cissus sicyoides	49 (2)	188 (9)	53 (3)	BDL	43 (2)	BDL	15.6 (0.8)	BDL
Costas spp.	57 (3)	18.5 (0.9)	49 (2)	7.6 (0.4)	49 (2)	9.2 (0.5)	27 (1)	3.8 (0.2)
Elaeis guianensis	58 (3)	48 (2)	48 (2)	7.4 (0.4)	54 (3)	7.8 (0.4)	31 (2)	BDL
Inga spp.	177 (9)	89 (4)	150 (8)	26 (1)	160 (8)	31 (2)	89 (4)	12.9 (0.6)
Melia azedarach	202 (10)	375 (19)	194 (10)	22 (1)	165 (8)	26 (1)	78 (4)	9.3 (0.5)
Musa spp.	23 (1)	114 (6)	24 (1)	BDL	24 (1)	4.8 (0.2)	14.4 (0.7)	BDL
Pachira aquatica	147 (7)	343 (17)	203 (10)	34 (2)	157 (8)	29 (1)	97 (5)	BDL
Spathodea campanulata	129 (6)	104 (5)	116 (6)	17.5 (0.9)	124 (6)	22 (1)	71 (4)	10.4 (0.5)
Eucalyptus camaldulensis	2138 (107)	755 (38)	1908 (95)	259 (13)	1471 (74)	289 (14)	824 (41)	113 (6)
Eucalyptus microtheca	1996 (100)	550 (27)	1825 (91)	274 (14)	1502 (75)	296 (15)	856 (43)	122 (6)
Eucalyptus papuana	345 (17)	218 (11)	313 (16)	47 (2)	269 (13)	51 (3)	145 (7)	20 (1)
Eucalyptus woodwardii	134 (7)	46 (2)	120 (6)	15.6 (0.8)	101 (5)	20 (1)	60 (3)	9.5 (0.5)
Pascopyrum smithii	3027 (151)	780 (39)	2642 (132)	382 (19)	2210 (111)	417 (21)	1192 (60)	169 (8)
Elymus elymoides	3805 (190)	1030 (51)	3275 (164)	463 (23)	2630 (131)	503 (25)	1438 (72)	202 (10)
Thinopyrum intermedium	818 (41)	268 (13)	714 (36)	100 (5)	583 (29)	109 (5)	307 (15)	43 (2)
Bouteloua gracilis	3509 (175)	974 (49)	3071 (154)	418 (21)	2419 (121)	454 (23)	1299 (65)	173 (9)
Sorghastrum nutans	2109 (105)	638 (32)	1816 (91)	251 (13)	1450 (72)	264 (13)	744 (37)	104 (5)

Table 40: Ash concentrations of Yb, Lu, Hf, W, Re, Pb, Th, and U. The reagent blank concentration of each trace metal analyzed was subtracted from the ash samples. *Costas spp.* and *Eucalyptus erythrocorys* were lost during sample processing.

Sample Name	Yb (ng)	Lu (ng)	Hf (ng)	W (ng)	Re (ng)	Pb (µg)	Th (ng)	U (µg)
Pinus ponderosa 1	408 (20)	59 (3)	276 (14)	564 (28)	44 (2)	4.9 (0.2)	986 (49)	0.34 (0.02)
Pinus ponderosa 2	779 (39)	113 (6)	493 (25)	706 (35)	104 (5)	6.1 (0.3)	2521 (126)	0.67 (0.03)
Pinus ponderosa 3	558 (28)	82 (4)	373 (19)	985 (49)	58 (3)	6.3 (0.3)	1849 (92)	0.5 (0.03)
Pinus ponderosa 4	555 (28)	82 (4)	396 (20)	517 (26)	53 (3)	6.3 (0.3)	1695 (85)	0.51 (0.03)
Arenga pinnata	54 (3)	BDL	320 (16)	540 (27)	350 (18)	221 (11)	173 (9)	4.5 (0.2)
Bambusa spp.	6.7 (0.3)	BDL	92 (5)	3764 (188)	206 (10)	1.81 (0.09)	59 (3)	0.028 (0.001)
Cissus sicyoides	15.5 (0.8)	BDL	92 (5)	14992 (750)	111 (6)	0.57 (0.03)	38 (2)	BDL
Costas spp.	27 (1)	3.7 (0.2)	20 (1)	51 (3)	0 (0)	0.5 (0.02)	28 (1)	0.033 (0.002)
Elaeis guianensis	15.9 (0.8)	BDL	158 (8)	2826 (141)	58 (3)	3.3 (0.2)	89 (4)	0.91 (0.05)
Inga spp.	80 (4)	10.4 (0.5)	76 (4)	440 (22)	66 (3)	0.98 (0.05)	209 (10)	0.79 (0.04)
Melia azedarach	47 (2)	7.7 (0.4)	246 (12)	2271 (114)	344 (17)	3.4 (0.2)	96 (5)	0.85 (0.04)
Musa spp.	4.5 (0.2)	BDL	56 (3)	327 (16)	251 (13)	0.85 (0.04)	0 (0)	1.67 (0.08)
Pachira aquatica	75 (4)	BDL	231 (12)	130 (6)	147 (7)	6.1 (0.3)	26 (1)	1.74 (0.09)
Spathodea campanulata	68 (3)	9.4 (0.5)	87 (4)	657 (33)	89 (4)	0.86 (0.04)	195 (10)	0.92 (0.05)
Eucalyptus camaldulensis	750 (37)	103 (5)	494 (25)	718 (36)	2921 (146)	4.8 (0.2)	2086 (104)	5 (0.3)
Eucalyptus microtheca	793 (40)	120 (6)	904 (45)	2008 (100)	5239 (262)	12.8 (0.6)	3370 (169)	3.1 (0.2)
Eucalyptus papuana	134 (7)	18.5 (0.9)	177 (9)	257 (13)	698 (35)	2.2 (0.1)	513 (26)	1.76 (0.09)
Eucalyptus woodwardii	66 (3)	10.2 (0.5)	176 (9)	0 (0)	267 (13)	2.3 (0.1)	243 (12)	0.183 (0.009)
Pascopyrum smithii	1115 (56)	154 (8)	1236 (62)	889 (44)	4.8 (0.2)	10.6 (0.5)	3146 (157)	0.86 (0.04)
Elymus elymoides	1283 (64)	177 (9)	1941 (97)	1656 (83)	97 (5)	12.5 (0.6)	4175 (209)	1.21 (0.06)
Thinopyrum intermedium	281 (14)	39 (2)	492 (25)	144 (7)	126 (6)	2.6 (0.1)	949 (47)	0.24 (0.01)
Bouteloua gracilis	1086 (54)	153 (8)	1452 (73)	394 (20)	0 (0)	13.2 (0.7)	3313 (166)	0.99 (0.05)
Sorghastrum nutans	680 (34)	92 (5)	1199 (60)	184 (9)	6.9 (0.3)	8 (0.4)	2748 (137)	0.65 (0.03)

APPENDIX I

PHOTOGRAPHS OF EXPERIMENTAL SETUP

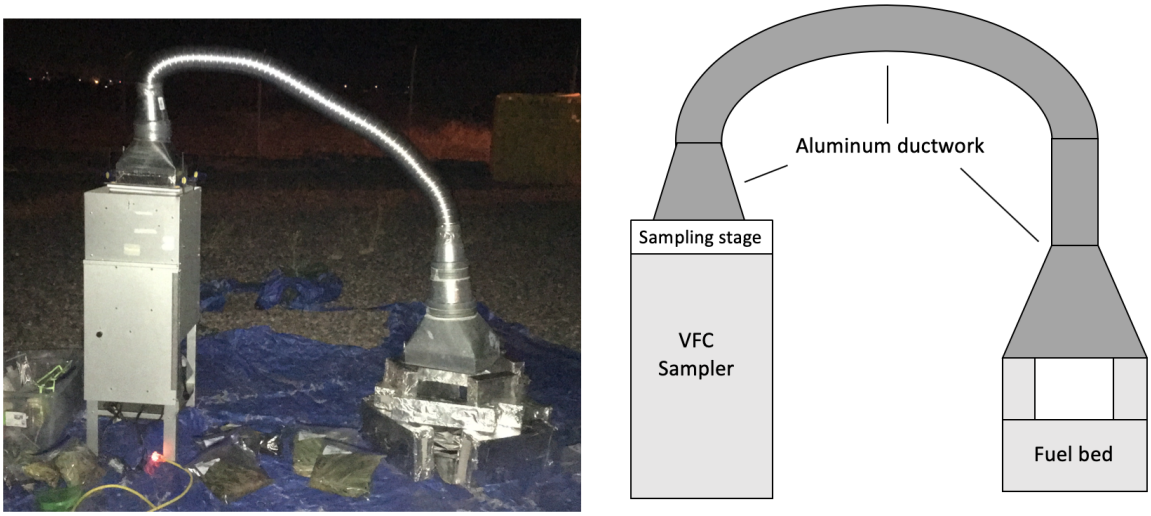

Figure 6: Burn experiment setup. Foliage was burned within the fuel bed (detailed in Figure 7), resulting combustion particles were drawn through the aluminum ductwork via the VFC sampler, and impacted clean cellulose filters at the sampling stage (Figure 8). Equipment was assembled upon a tarp to decrease soil entrainment during experiments.

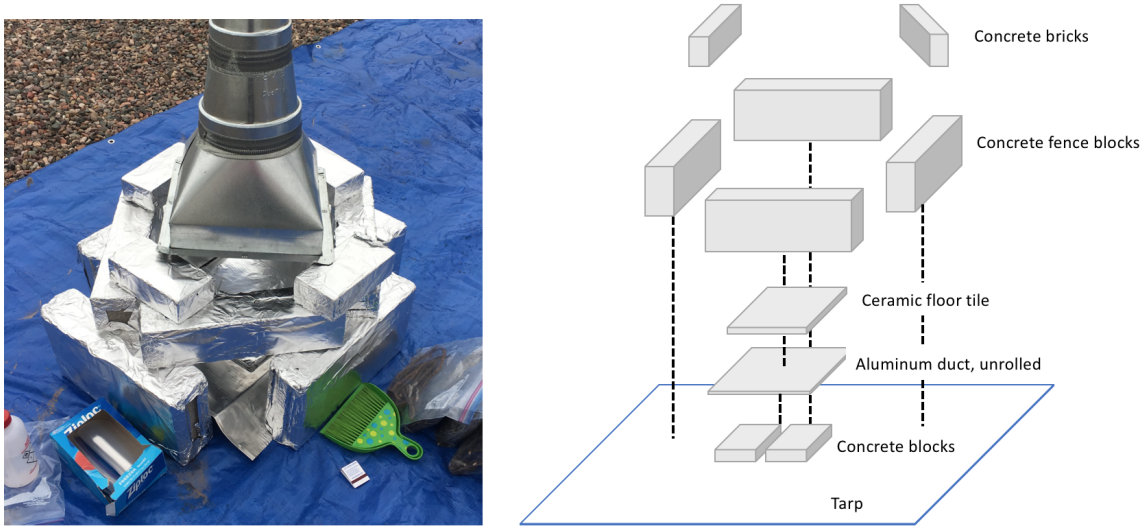

Figure 7: Contained fuel bed. Per fire marshal requirements, each burn was surrounded by aluminum foil-covered concrete blocks. To prevent tarp melting, the fuel bed consisted of an aluminum foil-covered ceramic floor tile on top of a 50 x 50 x 0.3 cm aluminum sheet and aluminum foil-covered ceramic blocks. The material for each burn was placed on top of a fresh piece of aluminum foil to prevent cross-contamination between samples and to facilitate the collection of post-burn ash.

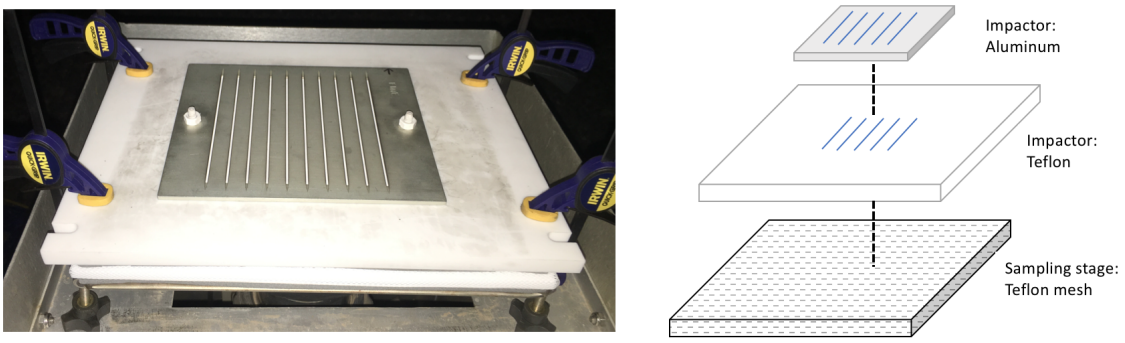

Figure 8: Sampling stage. To prevent contact between the filter and the steel mesh of the VFC sampler, the sampling stage was constructed with a polytetrafluoroethylene (PTFE, Teflon,) stage and impactor. PTFE and other plastic components were soaked in 20% trace metal grade HCl between each burn experiment. The aluminum impactor was cleaned before and after each burn using Kimwipes.